Dendritic signals from rat hippocampal CA1 pyramidal neurons during coincident pre- and post-synaptic activity: a combined voltage- and calcium-imaging study

Marco Canepari[1,2,3], Maja Djurisic[1,3] and Dejan Zecevic[1,3]

[1]*Department of Cellular and Molecular Physiology, Yale University School of Medicine, New Haven, CT 06520, USA*
[2]*National Institute for Medical Research, London, UK*
[3]*Marine Biological Laboratory, Woods Hole, MA 02543, USA*

The non-linear and spatially inhomogeneous interactions of dendritic membrane potential signals that represent the first step in the induction of activity-dependent long-term synaptic plasticity are not fully understood, particularly in dendritic regions which are beyond the reach of electrode measurements. We combined voltage-sensitive-dye recordings and Ca^{2+} imaging of hippocampal CA1 pyramidal neurons to study large regions of the dendritic arbor, including branches of small diameter (distal apical and oblique dendrites). Dendritic membrane potential transients were monitored at high spatial resolution and correlated with supra-linear $[Ca^{2+}]_i$ changes during one cycle of a repetitive patterned stimulation protocol that typically results in the induction of long-term potentiation (LTP). While the increase in the peak membrane depolarization during coincident pre- and post-synaptic activity was required for the induction of supra-linear $[Ca^{2+}]_i$ signals shown to be necessary for LTP, the change in the baseline-to-peak amplitude of the backpropagating dendritic action potential (bAP) was not critical in this process. At different dendritic locations, the baseline-to-peak amplitude of the bAP could be either increased, decreased or unaltered at sites where EPSP–AP pairing evoked supra-linear summation of $[Ca^{2+}]_i$ transients. We suggest that modulations in the bAP baseline-to-peak amplitude by local EPSPs act as a mechanism that brings the membrane potential into the optimal range for Ca^{2+} influx through NMDA receptors (0 to −15 mV); this may require either boosting or the reduction of the bAP, depending on the initial size of both signals.

(Resubmitted 16 November 2006; accepted after revision 30 January 2007; first published online 1 February 2007)
Corresponding author D. Zecevic: Department of Cellular and Molecular Physiology, Yale University School of Medicine, 333 Cedar Street, New Haven, CT 06520, USA. Email: dejan.zecevic@yale.edu

The concomitant activity of pre- and post-synaptic neurons can either potentiate or depress synaptic transmission in a persistent manner (e.g. Linden, 1999). These changes may be related to fundamental functions of the nervous system, including learning and memory (Bliss & Collingridge, 1993; Malenka & Nicoll, 1999). In many neurons, synchronized pre- and post-synaptic activity results in a large transient influx of calcium ions in synaptically active dendritic spines caused by the unblocking of NMDA receptors (NMDA-Rs) by the backpropagating action potential (bAP) (Malenka *et al.* 1988; Yuste & Denk, 1995; Koester & Sakmann, 1998). This calcium signal in spines, depending on its magnitude and dynamics, can then trigger postsynaptic biochemical processes responsible for different forms of NMDA-R-dependent associative long-term potentiation (LTP) (Sabatini *et al.* 2002; Raymond & Redman, 2006).

The non-linear interaction between the excitatory postsynaptic potentials (EPSPs) and bAPs which is responsible for the induction of LTP is not fully understood. This interaction depends critically on the amplitude of both signals (Pan & Colbert, 2001; Stuart & Hausser, 2001) and must therefore be spatially non-uniform. The test of this prediction requires spatially well-resolved measurements that have not been carried out because dendritic branches of small diameter are not accessible to electrode measurements.

Patch electrode recordings from one dendritic location on the main apical trunk in CA1 pyramidal neurons showed that $[Ca^{2+}]_i$ transients evoked by EPSP–AP pairing are correlated with supra-linear summation of electrical signals, termed boosting of the bAP baseline-to-peak amplitude (Watanabe *et al.* 2002). A similar boosting effect was found in the dendrites of both layer 5 (Williams &

 DOI: 10.1113/jphysiol.2006.125005

Stuart, 2000; Stuart & Hausser, 2001; Sjostrom & Hausser, 2006) and layer 2/3 (Waters *et al.* 2003) pyramidal cells in the neocortex. In all cases, the boosting of the dendritic action potentials was viewed as a mechanism potentially responsible for the precisely timed depolarization required for the unblocking of NMDA receptors to cause Ca^{2+} influx that is mandatory for the induction of LTP. However, although available evidence leaves no doubt that paired activity can amplify the size of bAPs in certain parts of the dendritic arbor, the question of whether boosting of the bAPs at the site of activated synapses is universally required for the induction of LTP is still open. An answer to that question would resolve whether or not LTP induced in the part of the dendritic arbor influenced by the bAPs is restricted to regions in which backpropagating sodium spike is boosted by preceding EPSPs. Alternatively, LTP induction could be dependent on paired activity but independent of bAP boosting. These two possibilities imply different functional structure of the dendritic arbor with regard to synaptic plasticity rules.

We combined voltage imaging and Ca^{2+} imaging from the same locations on the dendritic arbor of CA1 pyramidal neurons, including the oblique dendrites and thin apical branches, to characterize the relationship between electrical signals and related $[Ca^{2+}]_i$ transients during one cycle of the repetitive EPSP–AP pairing protocol that typically induces LTP. The results show that boosting of the bAP baseline-to-peak amplitude was not required for the supra-linear summation of calcium signals, and, by extrapolation, for LTP induction.

Methods

Slices, patch-clamp recording and intracellular application of dyes

All animal work was performed in accordance with the guidelines approved by Yale University Institutional Animal Care and Use Committee. Experiments were carried out on hippocampal slices from 21- to 30-day-old Sprague-Dawley rats. All measurements were carried out at 34–36°C. The rats were decapitated following halothane anaesthesia and 300 μm thick slices were cut in ice-cold solution using a custom-made rotary slicer with ceramic circular blade (Specialty Blades Inc., Staunton, VA, USA) rotating at 70 r.p.m. Slices were incubated at 37°C for 30 min and then maintained at room temperature (23–25°C). The extracellular solution used during slicing and recording contained (mM): 125 NaCl, 25 $NaHCO_3$, 20 glucose, 2.5 KCl, 1.25 NaH_2PO_4, 2 $CaCl_2$ and 1 $MgCl_2$, pH 7.4 when bubbled with a gas mixture (95% O_2, 5% CO_2). Somatic whole-cell recordings were made with 3–6 MΩ patch pipettes using a Multiclamp 700A amplifier (Axon Instruments Inc., Union City, CA, USA). The pipette solution contained (mM): 120 $KMeSO_4$, 10 NaCl, 4 Mg-ATP, 0.3 Tris-GTP, 14 Tris-phosphocreatine, 20 Hepes (pH 7.3, adjusted with KOH); 0.5 mg ml^{-1} of the voltage-sensitive dye JPW3028 and 300 μM of the calcium indicator dye bis-fura-2 ($K_d = 525$ nM at 1 mM Mg^{2+}, Invitrogen, Carlsbad, CA, USA). CA1 pyramidal cells were identified using infrared DIC video-microscopy on an upright microscope (Model BX51WI Olympus Inc., Japan).

Glass pipettes were first filled from the tip with dye-free solution by applying negative pressure for about 1 min and then back-filled with the solution containing the two indicator dyes. The dye JPW3028 was obtained from Leslie Loew and Joe Wuskell of the University of Connecticut. This is a doubly positively charged analogue of the ANEP series of lipophilic styryl dyes that is still sufficiently water soluble to be used for microinjection. Its close analogue (JPW1114; Zecevic, 1996) is available from Molecular Probes Inc. as D6923. Dye-free solution in the tip was necessary to prevent the leakage of the dye into the extracellular medium before the electrode is attached to the neuron. Intracellular staining was accomplished by free diffusion of the dyes into the soma in 15–60 min, depending on the electrode resistance. After diffusion of the dye into the soma was completed, as determined by measuring the resting light intensity from the soma, the patch-electrode with the dyes was detached from the neuron by forming an outside-out patch and the preparation was typically incubated for additional 1.5 h at room temperature to allow the voltage-sensitive dye to spread into distal processes. The spread of JPW3028 is relatively slow and apparently limited by its high affinity for lipid membranes. To obtain electrical recordings from the soma the cell body was repatched before making optical measurements.

The presynaptic axons were stimulated locally (5–50 μA; 150 μs) at a distance of 200–400 μm from the soma by an extracellular patch-electrode positioned close (< 10 μm) to a particular dendritic branch. We used $[Ca^{2+}]_i$ signals evoked by a train of five EPSPs to determine the position of the stimulating electrode that would result in the maximum localization of the evoked postsynaptic response. It was often possible to obtain $[Ca^{2+}]_i$ signals that were restricted to 5–10 pixels along a dendritic branch, corresponding to a dendritic length of 20–40 μm. Back-propagating APs were evoked by 2 ms current pulses to the soma. The pairing of EPSP and bAP signals was carried out using one cycle of a theta-burst pairing protocol. The cycle consisted of a train of five EPSPs paired with one bAP or a burst of two to five bAPs delivered at 100 Hz. The timing of EPSPs and bAPs was adjusted so that bAPs were evoked approximately at the peak of the EPSP recorded in the soma. When repeated many times, this patterned EPSP–AP pairing cycle is known to reliably induce LTP (Magee & Johnston, 1997; Frick *et al.* 2004). Optical recording experiments carried out during one EPSP–AP pairing cycle

represent a different set of experiments from the control electrode measurements of LTP induction following the entire theta-burst protocol. In these control experiments 10 bursts were repeated at theta-frequency (5 Hz) and this sequence was repeated three times at 0.1 Hz.

Optical recording

We used a stationary stage upright microscope equipped with two camera ports. One camera port had a standard high spatial resolution CCD camera for infrared DIC video-microscopy. The other camera port had a fast data acquisition camera with relatively low spatial resolution (80 × 80 pixels) but outstanding dynamic range (14 bits; NeuroCCD-SM, RedShirtImaging LLC, Decatur, GA, USA). The analysis and display of data were carried out using the NeuroPlex program (RedShirtImaging) written in IDL (ITT Visual Information Solutions, Boulder, CO, USA) running on an IBM-PC computer. The brain slice was placed on the stage of the microscope and the fluorescent image of the stained cell projected by a water immersion objective (60 ×, 1.0 NA; Nikon) via an optical coupler (0.09–0.11 ×; RedShirtImaging) onto the CCD chip. This objective was selected as a compromise between imaging area, spatial resolution and the signal-to-noise ratio (S/N). A 250 W xenon, short-gap arc lamp (Osram, XBO 250 W/CR ORF) powered by a low ripple power supply (Model 1700XT/A, Opti-Quip, Highland Mills, NY, USA) was the source of excitation light.

In voltage imaging, the best signals were obtained using an excitation interference filter of 520 ± 45 nm, a dichroic mirror with the central wavelength of 570 nm, and a 610 nm barrier filter (a Schott RG610). Membrane potential signals were recorded at a frame rate of 5 kHz. With the sensitivity of the intracellular voltage-sensitive dyes used (1–6% $\Delta F/F$ per 100 mV in recording from dendritic processes), relatively good signal-to-noise ratios could be obtained in single-trial recordings with modest spatial averaging (4–10 pixels) from dendritic regions that were about 300 μm away from the soma. Modest signal averaging (4 trials) was used to improve the signal-to-noise ratio further. The peak amplitude of the optically recorded bAP in single trials was systematically underestimated by 5 ± 3%, as determined by comparing electrically and optically recorded signals from neighbouring locations (soma and proximal dendrite) – this was the effect of a slight under-sampling of action potential signals at 5 kHz. This error was reduced by averaging action potential signals using the peak of the recorded spike as the reference data point for averaging optical traces (see below). Additionally, because this error applies to both unpaired and paired signals, the data were not corrected and the signals were directly compared. Slow changes in light intensity due to bleaching of the dye were corrected by subtracting an appropriate exponential function derived from the recording trials with no stimulation. The residual slow changes in baseline after bleaching correction, if present, had no effect on baseline-to-peak amplitude of bAPs because they were small and approximately 100 times slower than the rising phase of an action potential.

The conclusions derived from our measurements are based on the direct comparison of optical signals recorded from same dendritic locations under different conditions. Such a comparison is valid only if the light intensity is linearly proportional to the membrane potential over the entire range of signal amplitudes. This has been documented for a wide range of membrane potential transients (−100 to +100 mV) in the early work on voltage-sensitive dyes (Ross *et al.* 1977; Wu & Cohen, 1993) and confirmed in a detailed study on biophysical properties of amino-styryl dyes that we used in our measurements (Loew *et al.* 1992). Also, the same dye has been shown to track the full-size action potential exactly in several neuronal types (Zecevic, 1996; Antic *et al.* 1999; Antic, 2003; Djurisic *et al.* 2004; Palmer & Stuart, 2006), a result that implies a strictly linear relationship between the dye signal and the membrane potential in the entire physiological range.

Ca^{2+} signals were recorded at the frame rate of 500 Hz using an excitation interference filter of 380 ± 15 nm, a dichroic mirror with central wavelength of 400 nm and a 450 nm barrier filter; four trials for each stimulation protocol were averaged to improve the signal-to-noise ratio. Calcium fluorescence transients are expressed as $-\Delta F/F = (F_0 - F)/F_0$, where F is the fluorescence and F_0 is the resting fluorescence. The value of F was calculated after subtracting auto-fluorescence determined for an area far from the loaded dendrite. Due to uneven illumination of the field of view and due to differences in auto-fluorescence between different parts of the slice, background fluorescence values varied between different regions on the same slice by a factor of up to 2.8. However, because we compared signals from the same dendritic regions under different conditions, possible errors in calculating $\Delta F/F$ introduced by uncertainties about actual contribution of auto-fluorescence to the light intensity from the stained neuron do not influence conclusions from our measurements. Bis-fura-2 (300 μM) was chosen to maximize the S/N of Ca^{2+} fluorescence signals. At this concentration (total dye buffer capacity of ∼571) bis-fura-2 will dominate over the endogenous buffers by an order of magnitude (Neher & Augustine, 1992; Helmchen *et al.* 1996; Maravall *et al.* 2000). In these conditions the $\Delta F/F$ calcium signal should be proportional to the total increase in Ca^{2+} evoked by bAPs (Sabatini *et al.* 2002; Nevian & Sakmann, 2004). As a test for linearity we recorded Ca^{2+} signals related to individual bAPs during a short burst of three spikes evoked at a frequency of 100 Hz (Supplemental Fig. 1). The amplitude of the optical signal related to the first

bAP in a sequence was compared to amplitudes of the Ca^{2+} signals corresponding to the second and the third bAP. The results show no significant difference between groups (paired t test; $P > 0.4$; $n = 6$) suggesting that an approximately linear relationship between $\Delta F/F$ and free Ca^{2+} concentration can be assumed in measurements of bAP signals.

Pharmacological effects and photodynamic damage

$[Ca^{2+}]_i$ indicator. Loading of neurons with bis-fura-2 did not have detectable pharmacological effects (toxicity of the indicator dye in the absence of excitation light) on electrical behaviour of neurons. During calcium imaging, the exposure of the preparation to the excitation light was limited to the recording periods of 400 ms. We did not detect any change in the amplitude or the time course of optical or electrical signals due to possible photodynamic damage (toxicity induced by the interaction of the indicator dye with high intensity light) after 50–100 recording trials that were typically collected during one experiment.

Membrane potential indicator. The toxicity of voltage-sensitive dyes is less well established compared with $[Ca^{2+}]_i$ indicators. Previous studies have shown that the voltage-sensitive dyes used (JPW 1114 or JPW 3028) have little or no pharmacological effect when applied at functional concentrations to both invertebrate (Antic & Zecevic, 1995; Antic *et al.* 2000) and vertebrate neurons (Antic *et al.* 1999; Antic, 2003; Djurisic *et al.* 2004; Palmer & Stuart, 2006). We obtained the same result in CA1 pyramidal neurons. Action potential amplitude, voltage threshold and the width at half-height were recorded in neurons at the beginning of the staining period and after repatching the same neuron following equilibration of the dye inside the cell. The staining and equilibration periods together lasted approximately 2.5 h. There was no statistically significant effect on AP amplitude (control 101 ± 5.2 mV *versus* 98 ± 4.5 mV stained), voltage threshold (control $13.2 \pm 1.9.0$ mV depolarized to rest *versus* 14.5 ± 1.1 mV stained), or the width at half-height (control 0.67 ± 0.02 ms *versus* 0.71 ± 0.03 ms stained) ($n = 4$, $P > 0.2$) (Fig. 1*A* and *B*).

Previous studies have also shown, for invertebrate neurons, rat neocortical layer V pyramidal neurons and mitral cells of the olfactory bulb, that photodynamic damage during optical recording was not present if the exposures of the dendritic arbor to excitation light were kept relatively short (100 ms) and if successive trials were separated by dark intervals lasting several minutes (Zecevic, 1996; Antic *et al.* 1999; Antic, 2003; Djurisic *et al.* 2004). Since our experiments were designed to determine the effect of EPSP–bAP pairing on the size and shape of the bAPs, it was critical to establish directly for the dendrites of CA1 pyramidal neurons whether photodynamic damage caused any non-specific alterations in the properties of bAPs. A typical experiment in this study required no more than 8–16 recording trials (illumination time: 100–150 ms per trial). In every experiment that involved voltage imaging we compared the very first single-trial optical recording of the bAP evoked alone (control signal) with the last bAP signal at the end of the experiment. The results indicated that the first and the last optical recording of the evoked bAP from a selected region on the dendritic arbor were identical (allowing for the noise in the recording). Optical measurements from distal dendritic regions typically showed bAPs with a fast and a slow component of the repolarizing phase (Fig. 1*C* and *D*) in agreement with numerous dendritic electrode recordings (e.g. Fig. 7A in Bernard & Johnston, 2003). The average bAP signal amplitude, derived from experiments that included 8–16 single-trial recordings from 38 neurons, at the end of the experiment was $99.6 \pm 0.5\%$ as big as the first optical signal (Fig. 1*C* and *E*). Clearly, 16 recording trials had no effect on the electrical properties of the dendritic tree, and the limit in the number of recording trials set by the photodynamic damage might be substantially higher. It was not simple to determine this parameter because large number of recordings carried out at low repetition rate (1 trial every 2 min) requires that the results are corrected for a non-specific run-down effect which varies between different neurons due to many factors. This analysis was not carried out. However, we compared optical bAP signals from five experiments in which 30–52 individual trials were recorded (Fig. 1*D* and *E*). The results showed that, on average, the last bAP signal amplitude was $100.6 \pm 1.8\%$ compared with the first optical signal recorded at the start of the experiment. The first and the last recording of V_m signals were separated by 60–140 min in different experiments. Using optical recording to determine the stability of dendritic membrane potential signals during such an extended period of time is precise and has an advantage over patch-electrode recording because it is not prone to errors due to common increase in the access resistance of the dendritic patch-electrode which, together with the electrode capacitance, acts as an RC filter decreasing the amplitude and increasing the width of the bAP (Waters *et al.* 2005).

Recently, another laboratory used the same voltage-sensitive dye and the same experimental protocol to study AP initiation in the axon of cortical layer 5 pyramidal neurons (Palmer & Stuart, 2006). Their results corroborated our conclusion that the voltage-sensitive dye had minimal photo-toxic effects.

We also carried out control measurements to test whether the voltage-sensitive dye interferes with spine mechanisms that mediate the induction of LTP. In this set of experiments, LTP was induced using a

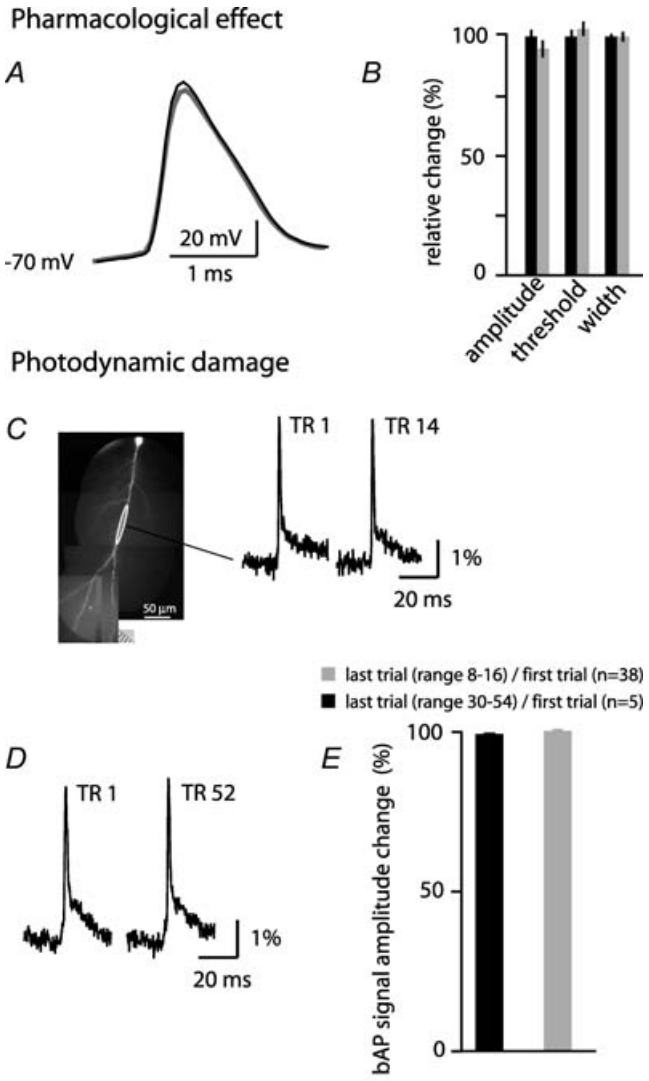

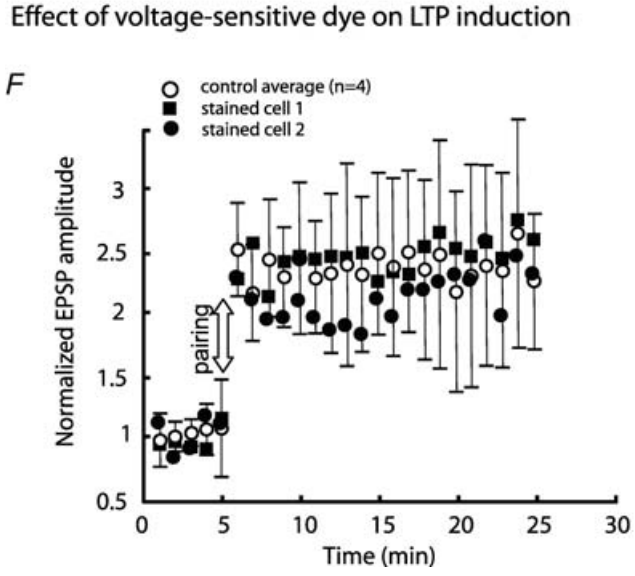

complete theta-burst pairing protocol described above. The measurements were carried out in four control neurons and two pyramidal cells that were loaded with the voltage-sensitive dye using the standard staining procedure (without bis-fura-2), including a 90 min incubation at room temperature to allow for dye equilibration in dendritic processes. A robust LTP was induced in both control and stained neurons indicating little or no pharmacological effect of the dye. Figure 1*F* shows the average magnitude and the time course of induced LTP for control neurons ($n = 4$) and the data for the two stained neurons. Data for stained neurons obviously overlapped with the control measurements indicating little or no effect of the dye on LTP induction.

Results

We explored the dendritic V_m and $[Ca^{2+}]_i$ signals evoked by localized EPSPs, by bAPs, and by paired activity following a stimulation pattern that corresponds to one cycle of the repetitive theta-burst protocol that typically induces associative LTP (Magee & Johnston, 1997; Frick *et al.* 2004; Raymond & Redman, 2006). Changes in membrane potential and in $[Ca^{2+}]_i$ were recorded sequentially from the dendritic tree of the same neuron as fractional changes in fluorescence intensity using two different filter sets and a fast CCD camera. EPSPs were evoked at a distance of 220–400 μm from the soma by an extracellular patch-electrode positioned close to a particular dendritic branch ($< 10\,\mu$m). The stimulus intensity was adjusted so that the amplitude of the first EPSP recorded in the soma was in the range of 1–5 mV and

Figure 1. Pharmacological effects and photodynamic damage of the voltage-sensitive dye
A, electrode recordings from the soma. The resting membrane potential and AP shape and size were not altered significantly after the 40 min staining period and additional 90 min of incubation at room temperature (dye equilibration time; grey trace) from the original values at the start of the recording (black trace). *B*, summary data for spike amplitude, voltage threshold, and width at half-height determined for 4 neurons before (black bars) and after (grey bars) staining and dye equilibration. The differences were not statistically significant. *C*, the 1st and the 14th 100 ms optical recording trial (TR 1 and TR 14) of the evoked bAP signals from a selected region (white circle) on the dendritic arbor of a stained neuron shown on the left. *D*, the 1st and the 52nd 100 ms optical recording trial of the evoked bAP signals from the dendritic arbor of another stained neuron. *E*, relative change in the amplitude of the last single-trial recording of the bAP signal normalized to the size of the first recording shown for two groups of experiments. In one group (black bars) the total number of trials was in the range of 8–16 in different experiments ($n = 38$). In the other group the total number of trials was in the range of 30–54 in different experiments ($n = 5$). The differences were not statistically significant. *F*, normalized EPSP amplitude before and after paired stimulation showing the average magnitude and the time course of LTP for control neurons ($n = 4$) and the data for two neurons stained with the voltage-sensitive dye. Error bars are S.D. values.

the total depolarization following a train of five EPSPs at 10 ms intervals was in the range of 10–20 mV. Postsynaptic action potentials were evoked by 2 ms current injections to the soma via a patch-electrode.

First, we established that for both voltage and calcium signals repeated application of the same stimulation protocol, separated by several minutes, resulted in the same response. Figure 2 shows the V_m signal and the $[Ca^{2+}]_i$ signal recorded from one location on an oblique dendrite in response to paired stimulation. The results show that signals were practically identical in repetitive trials (allowing for the variability typical for the statistical nature of synaptic transmission in these neurons; Bekkers & Stevens, 1990). Therefore, it was possible to directly compare V_m signals and $[Ca^{2+}]_i$ signals recorded sequentially.

Figure 3 is an example of typical measurements carried out to correlate V_m signals with the corresponding change in $[Ca^{2+}]_i$ at the site of activated synapses. V_m signals and $[Ca^{2+}]_i$ transients were monitored during three stimulation protocols (bAPs alone, EPSPs alone, paired stimulation) from multiple sites on a dendritic tree. The recordings from one location on an oblique dendrite close to a stimulating electrode revealed a marked localized supra-linear increase in the $[Ca^{2+}]_i$ signal evoked by pairing a train of EPSPs with a burst of two bAPs (Fig. 3*C*; middle set of traces). At the same time, a dramatic reduction in the baseline-to-peak bAP amplitude was observed during the paired stimulation. The reduction in the size of the bAP during paired activity is illustrated in Fig. 3*D*. The spike signals corresponding to bAPs evoked alone and during paired activity are superimposed on the baseline membrane potential before the EPSP train (upper traces) and on the baseline membrane potential immediately preceding the spikes evoked during the last two EPSPs in a train (lower traces). Optical signals in Fig. 3*C* and *D* were obtained by averaging four individual trials, as shown in Fig. 3*E*, to improve the signal-to-noise ratio and confirm that the response was consistent over repeated measurements. During averaging, recordings of bAP signals were alternated with recordings of paired activity. In this and all other experiments, optical signals were averaged offline separately for every action potential in a burst using the peak of the spike as the reference data point for averaging to avoid the effect of temporal jitter (Fig. 3*E*). This initial result showed clearly that a supra-linear increase in $[Ca^{2+}]_i$ that serves as a trigger for LTP induction did not require boosting in bAP baseline-to-peak amplitude and was, in fact, present even though the bAP itself was markedly reduced in amplitude by paired activity. In this experiment, the additional depolarization provided by the reduced bAPs was modest, suggesting that similar depolarization and associated supra-linear increase in $[Ca^{2+}]_i$ might be produced by a more intense EPSP train alone. The ability of local depolarization driven by subthreshold EPSP trains of different amplitude to generate supra-linear increase in $[Ca^{2+}]_i$ comparable to those evoked by paired activity was

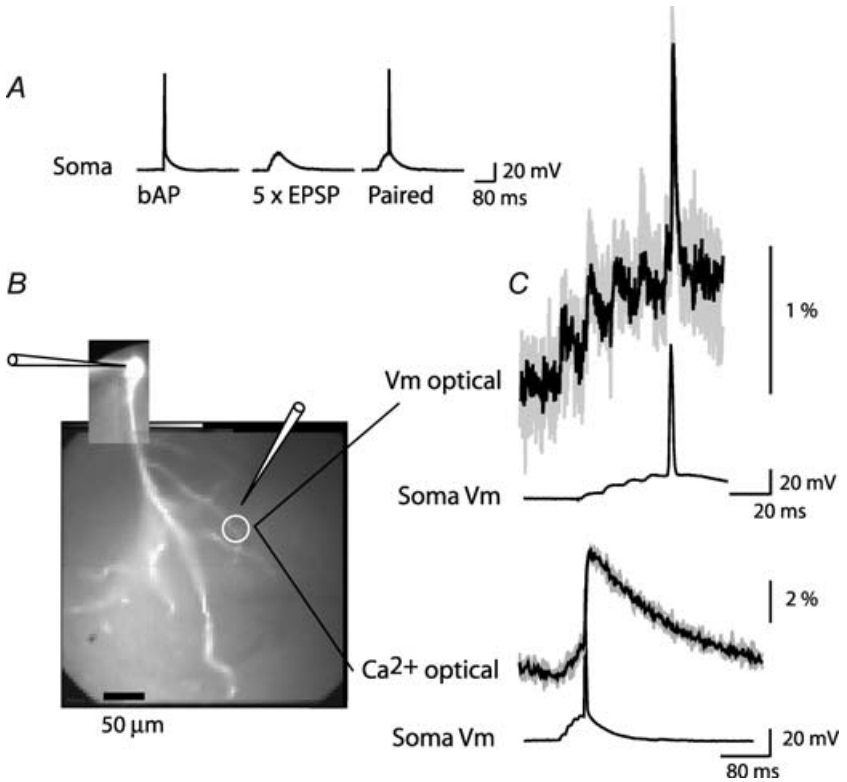

Figure 2. V_m and $[Ca^{2+}]_i$ signals in response to repeated stimulation are stable
A, electrical recordings from the soma during evoked bAP, evoked train of 5 EPSPs, and paired stimulation. *B*, fluorescent image of a CA1 pyramidal neuron (bis-fura-2 excitation); white circle indicates recording location; somatic patch-electrode and extracellular electrode are shown schematically. *C*, optical recording of local V_m and $[Ca^{2+}]_i$ signals in response to repeated application of paired stimulation. Four recording trials (grey) and an average result (black) are superimposed for both signals. Note the difference in the time scale.

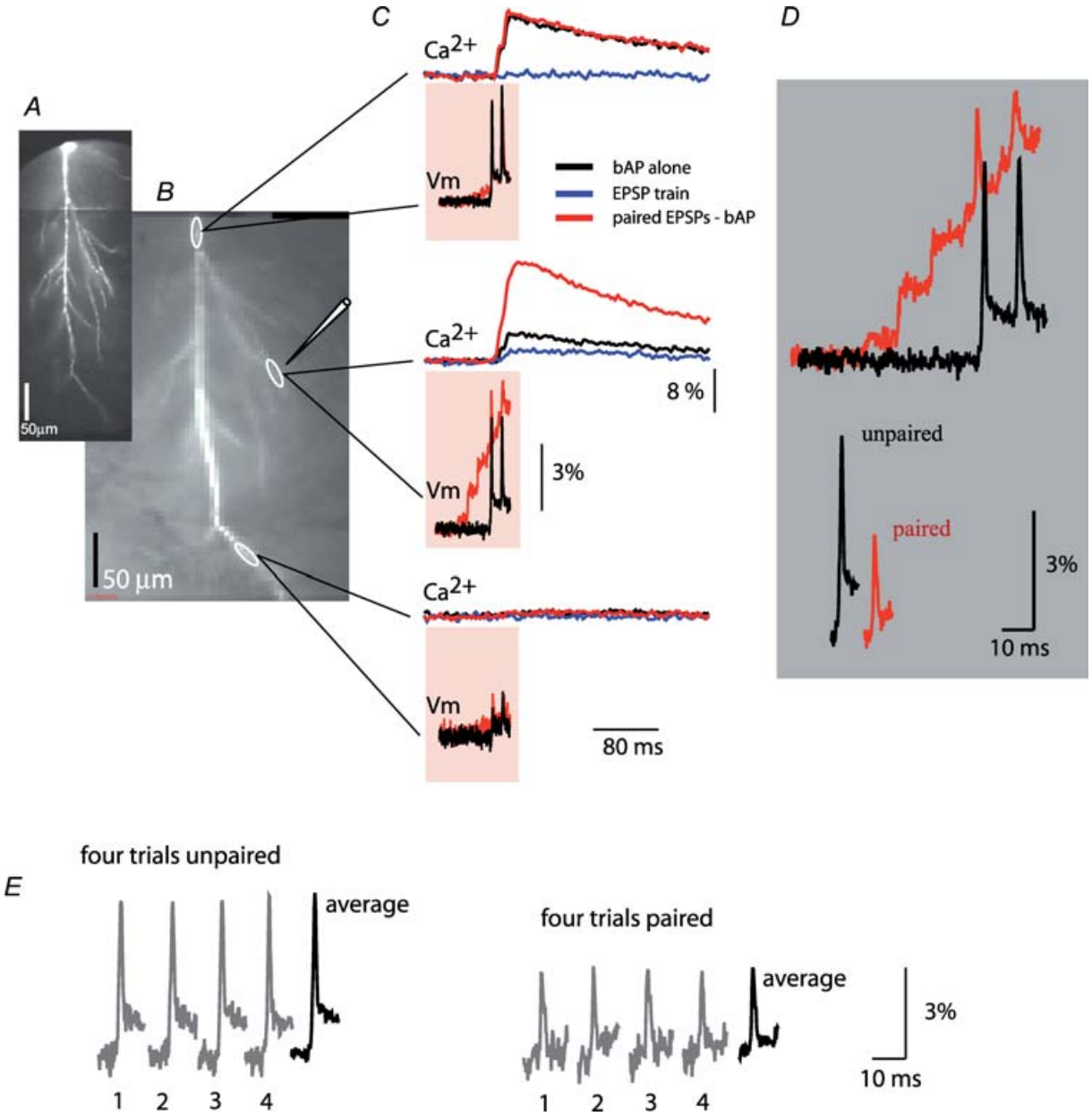

Figure 3. Comparison of V_m and $[Ca^{2+}]_i$ signals from same dendritic locations
A, a composite image of a neuron (voltage-sensitive dye excitation). *B*, low resolution images (bis-fura-2 excitation) of the dendritic arbor in recording position. Representative recording locations marked by white ovals; the position of the extracellular electrode shown schematically. *C*, V_m signals and $[Ca^{2+}]_i$ signals related to bAP (black traces), EPSP train (blue traces, shown only for $[Ca^{2+}]_i$ signals), and paired EPSP–AP activity (red traces). V_m signals (100 ms) during paired activity are superimposed with the recordings of bAP signals alone. Calcium recordings (400 ms) are shown above V_m traces – signals during three stimulation protocols (bAPs, EPSP train, paired) are superimposed. *D*, V_m recordings of the first bAP on the expanded time scale superimposed on the same baseline to show region-specific changes in the peak membrane depolarization during paired activity (upper traces). Lower traces: spike signals aligned to indicate the difference in baseline-to-peak amplitude (EPSP signal subtracted). Traces are shifted horizontally with respect to each other for clarity. *E*, V_m signal amplitude comparison: four trials were averaged for both paired and unpaired stimulation pattern. The peak of the relevant spike was used as the reference time point for averaging to remove the effect of trial-to-trial temporal jitter in the timing of AP generation on the shape and size of the averaged signal. In all experiments individual trials were inspected to verify that averaging did not introduce errors.

not tested. However, previous work speaks against that possibility (Magee & Johnston, 1997; Chang & Jackson, 2006) by providing strong evidence that LTP in the hippocampal slice depended critically on the generation of postsynaptic spikes during the induction protocol.

We carried out a series of experiments to explore the spatial characteristics of bAP amplitude modulation induced by concomitant subthreshold EPSPs. The electrical, V_m signal were spatially and temporally correlated with the associated NMDA-dependent component of the $[Ca^{2+}]_i$ signal known to be mandatory for LTP induction. This component was determined using 2-amino-5-phosphonopentanoic acid (AP-5) to block NMDA receptor current.

Ca^{2+} signals from bAPs, EPSP trains and paired pre- and post-synaptic stimulation

The calcium measurements were carried out first. The results showed that $[Ca^{2+}]_i$ signals related to bAPs evoked alone declined in amplitude with distance from the soma and became undetectable in dendritic regions that were more than 300–400 μm away from the cell body. Figure 4*A*, top panel, bAP, is a typical example of the colour-coded relative spatial map of the bAP-driven $[Ca^{2+}]_i$ signal; recordings from four selected locations are shown on the right of the colour-coded display. In all measurements the calcium signals clearly declined with distance from the soma. Our measurements are consistent with previous studies showing that the amplitude of the bAPs, as well as the associated $[Ca^{2+}]_i$ transients mediated by voltage-sensitive calcium channels (VSCC), declined monotonically with distance from the soma along the distal part ($< 200\ \mu$m from soma) of the main apical dendrite (Jaffe *et al.* 1992; Spruston *et al.* 1995; Frick *et al.* 2004).

We next recorded $[Ca^{2+}]_i$ signals evoked by a train of five EPSPs generated at 100 Hz by local extracellular stimulation of presynaptic axons. Figure 4*A*, second panel from top, shows typical recordings. The major component of the EPSP signal evoked by focal electrical stimulation was localized to a small region on a dendritic branch adjacent to the stimulating electrode. Spatial distribution of the EPSP signal is shown as a relative colour-coded map; the recordings from four selected regions are shown on the right.

The experiment was continued to measure $[Ca^{2+}]_i$ signals during paired pre- and post-synaptic activity known to induce non-linear effects that are crucial for the triggering of LTP. Paired activity (Fig. 4*A*, Paired, third panel from top) resulted in simple, linear summation of $[Ca^{2+}]_i$ signals in some dendritic regions (e.g. locations 1) and a marked supra-linear summation at other sites (locations 2 and 3). To isolate the supra-linear component of $[Ca^{2+}]_i$ transients and to determine its spatial distribution, the bAP $[Ca^{2+}]_i$ signal and the EPSP $[Ca^{2+}]_i$ signal were subtracted from the total $[Ca^{2+}]_i$ transient evoked by paired stimulation – the residual signal represents the supra-linear component. The relative spatial map of this component is shown in Fig. 4*A* (Supra-linear Ca^{2+}, bottom panel). The recordings of the subtracted results from the four locations are shown on the right. In this experiment, the spatial distribution of the supra-linear component of the $[Ca^{2+}]_i$ signal is wider than the spatial distribution of the Ca^{2+} transient recorded in response to EPSP train evoked alone. This result indicates that a fraction of the supra-linear increase in $[Ca^{2+}]$ is not related to Ca^{2+} influx through NMDA-Rs of activated synapses but most probably results from opening of VSCCs in response to depolarization caused by paired activity.

The sensitivity of calcium recordings allowed clear resolution and quantitative comparison of different components of the dendritic $[Ca^{2+}]_i$ signals related to three stimulation protocols (bAPs, train of EPSPs, paired activity). The comparison of soma V_m signals and $[Ca^{2+}]_i$ signals recorded from the stimulation site (location 3) during different stimulation protocols is shown in Fig. 4*B*. The result from this type of measurements from 19 neurons showed that the supra-linear component of the $[Ca^{2+}]_i$ transient always had the largest amplitude at the EPSP stimulation site. The average amplitude of this component, normalized to the computed sum of the bAP and EPSP calcium signals recorded separately, was $175 \pm 15\%$ (S.E.M., $n = 19$). A plot of the summary result is shown in Fig. 4*C*.

Membrane potential signals

V_m signals related to bAPs evoked alone and paired with a train of EPSPs were recorded from the same regions on the dendritic tree. We looked for a critical V_m signal that could be responsible for the supra-linear Ca^{2+} signal. A typical result is illustrated in Fig. 4*D*. The top panel shows the spatial distribution of the bAP signal amplitude in a colour-coded display together with the recordings from four locations. The amplitude of V_m signals from different locations can be compared only approximately because the optical signals could not be calibrated in terms of membrane potential changes (Djurisic *et al.* 2004). However, the calibration of voltage-sensitive dye signals in terms of the absolute value of membrane potential (in mV) is not critical for this study – our conclusions are based on the comparison of signals recorded from same locations under different conditions.

Even though the calibration of optical signals can only be approximated, our measurements are in general agreement with numerous dendritic electrical recordings described by others – in the distal parts of the dendritic tree the amplitude of the bAP signal declined monotonically with distance from the soma. In the experiment

shown in the Fig. 4, the amplitude of bAP declined below the resolution of our measurements at a distance of approximately 350 μm from the cell body, a result consistent with previous studies (Bernard & Johnston, 2003; Frick *et al.* 2004). A similar decline in bAP amplitude with distance from the soma was obtained from all neurons tested ($n = 38$).

Changes in peak membrane depolarization induced by paired activity

Comparison of the signal size from the same dendritic regions during unpaired and paired activity was the core of the analysis of the relationship between V_m signals and associated supra-linear $[Ca^{2+}]_i$ transients.

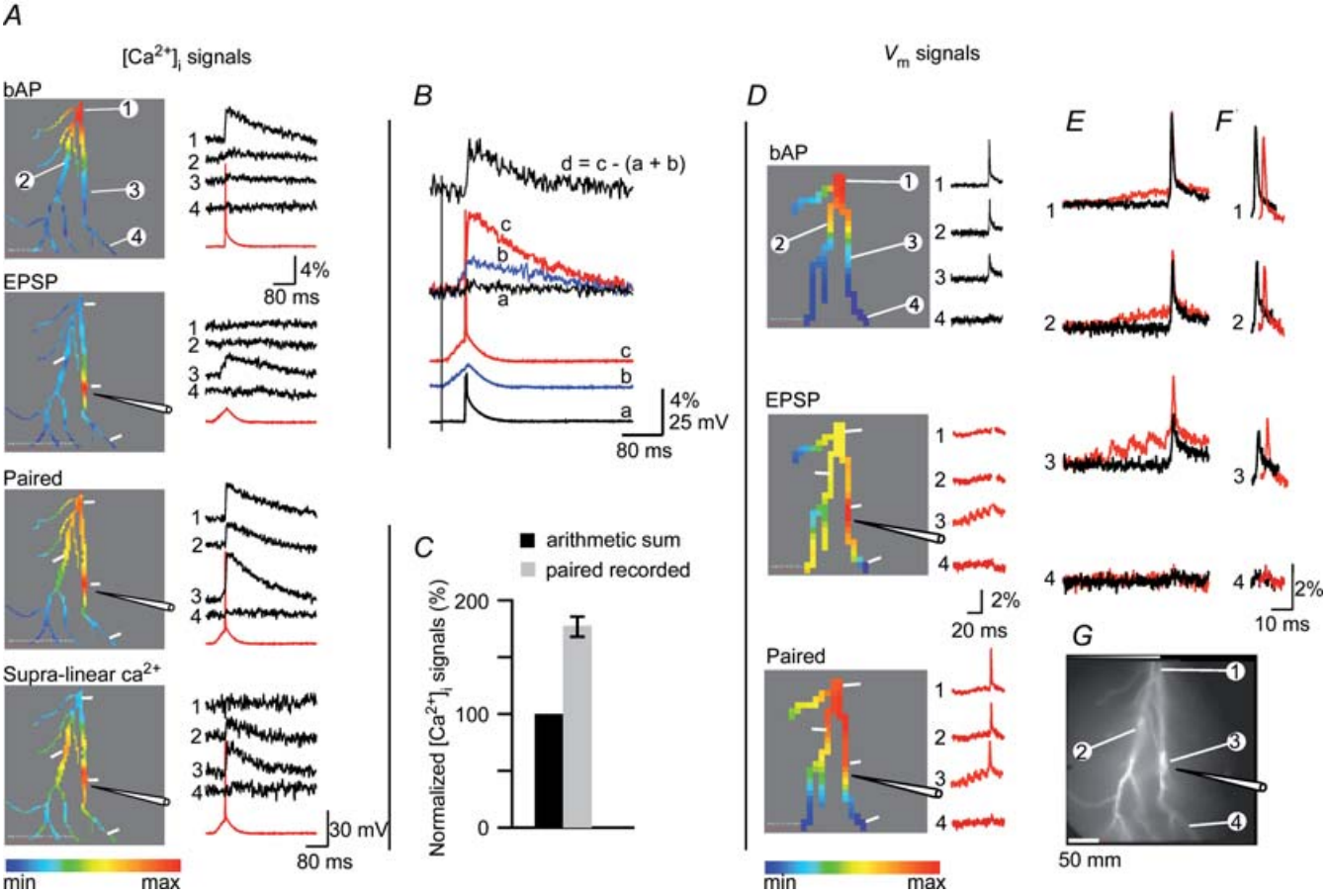

Figure 4. Supra-linear component of the dendritic calcium signal is spatially and temporally correlated with the increase in the peak membrane depolarization evoked by paired activity
A, calcium signals: the spatial maps of the peak $[Ca^{2+}]_i$ transient evoked by the three stimulation protocols shown in the colour-coded display on the left. Corresponding signals from four representative locations (indicated in the top panel) are shown on the right (red traces – somatic V_m recording). In this and all subsequent figures, the relative colour coding (minimum-to-maximum signal amplitude) was applied separately to each measurement. A mask was applied (with the threshold set to 200% of the average background light intensity) that revealed only detectors that received light from the stained neuron. The bottom panel (Supra-linear Ca^{2+}) shows the relative spatial map and the recordings of the supra-linear component of the $[Ca^{2+}]_i$ signal during paired activity. *B*, comparison of the somatic V_m recordings (lower 3 traces; AP truncated in *a*) and calcium signals at the stimulation site (upper 4 traces) in response to bAP (black), a train of 5 EPSPs (blue) and paired activity (red). The trace on top is the isolated supra-linear component of the $[Ca^{2+}]_i$ signal marked *d*. *C*, summary result ($n = 19$): supra-linear component of the $[Ca^{2+}]_i$ signal at the stimulation site (grey bar) normalized to the sum of the bAP and EPSP calcium signals (black bar). On average, 43% of the total calcium signal was the result of the non-linear increase in Ca^{2+} influx during paired activity. *D*, V_m signals: the relative spatial maps constructed for the peak of the bAP, EPSP train and paired activity shown in the colour-coded displays on the left; corresponding signals from 4 locations are shown on the right. In the middle panel (EPSP), spike signals were removed artificially to isolate parts of the recording used to generate a spatial map of the peak EPSP signal alone. *E*, bAP signals superimposed on the same baseline with paired EPSP–bAP signals to reveal region-specific changes in the peak membrane depolarization. *F*, bAP signals aligned with paired EPSP–bAP signals to reveal region-specific differences in action potential baseline-to-peak amplitudes (EPSP signals subtracted). Traces are shifted horizontally with respect to each other for clarity. *G*, a fluorescence image of the CA1 pyramidal neuron (bis-fura-2 excitation).

The comparison was carried out after recording the membrane potential signals initiated by pairing bAPs with a train of locally evoked EPSPs. The example illustrated in Fig. 4*D–F* shows that the peak depolarization, at the site of EPSP origin (location 3), was larger during paired activity compared with bAP evoked alone. This effect was the most pronounced at the stimulated site, but other locations were also affected as a result of the passive spread of the EPSPs (e.g. locations 1 and 2). The increase in the peak membrane depolarization at the site of the activated synapse induced by paired activity was recorded without exception in all cells ($n = 38$). Spatially, the largest increase was correlated with the NMDA-R-dependent supra-linear $[Ca^{2+}]_i$ signal at the stimulation site. The relationship between the increase in the peak membrane depolarization and the NMDA-R-dependent supra-linear $[Ca^{2+}]_i$ signal was analysed in 13 neurons in which the NMDA-R-dependent $[Ca^{2+}]_i$ signal was isolated using AP-5 and will be described later, along with the effects of AP-5.

Changes in baseline-to-peak bAP amplitude induced by paired activity

In the experiment shown in Fig. 4, the baseline-to-peak amplitude of the bAP at the stimulation site (location 3) was boosted by 21% during paired activity (Fig. 4*F*). This result is in agreement with previous measurements showing a similar effect recorded electrically from regions on the main apical trunk about 250–300 μm distal from the soma (Magee & Johnston, 1997; Watanabe *et al.* 2002). However, at two other sites (locations 1 and 2) the amplitude of the bAP was slightly suppressed. We analysed the results from experiments on 38 neurons (44 stimulation sites) to determine the effect of pairing on bAP amplitude. The result indicated that, in different neurons as well as at different locations in the same dendritic arbor, the bAP paired with the train of EPSPs and measured at the site of activated synapses, was either boosted, unaltered, or suppressed, compared with the bAP evoked alone (the quantitative analysis and the summary plot is given below). At a given location, however, the effect was stable in repeated measurements. The experiment shown in Fig. 5 (same cell as in Fig. 3) is an example of a striking reduction in the baseline-to-peak amplitude of bAPs in an oblique dendrite evoked by paired activity. In this neuron the evoked supra-linear increase in the $[Ca^{2+}]_i$ transient during paired activity at the stimulation site (location 3) was accompanied by a suppression of bAP amplitude (first bAP reduced by 50%; Fig. 5*C*) even though the peak depolarization increased by 35%. This result is in contrast to the boosting effect of pairing in the experiment shown in Fig. 4 and in experiments reported by others (Magee & Johnston, 1997; Watanabe *et al.* 2002). At the same time, at an adjacent site on the apical trunk (location 4), the first spike was boosted in amplitude by 17% during paired activity but supra-linear summation of the calcium signal was absent at that location.

The change in the baseline-to-peak amplitude of bAPs had different polarity in measurements from different dendritic sites. To describe the effect, we constructed a frequency distribution histogram (Fig. 5*E*) for the effect of pairing on bAP baseline-to-peak amplitude. The frequency distribution histogram demonstrated that the effect measured at different stimulation sites in the dendritic arbor of different neurons varied from 'depressed' to 'boosted' ($n = 44$). In 17 neurons the baseline-to-peak bAP amplitude was boosted at the site of synaptic stimulation, in 18 neurons it was depressed and in 9 neurons it either did not change with paired activity or the possible change was below recording resolution. Clearly, the type of interaction between EPSP and bAP was region-specific.

In 12 neurons of the boosted group, the stimulation site was on the apical dendrite, at a distance that ranged from 220 to 350 μm from the soma in different experiments. In the remaining 5 cells, including the experiments shown in Fig. 4, the stimulating electrode was positioned either on an oblique dendrite or on a dendritic branch that was distal to the primary bifurcation of the apical trunk. The average boosting of the bAP amplitude was determined separately in these two groups of cells. The difference was not significant ($P > 0.2$, two-population t test) showing that the effect was not specific for one type of dendritic branches. Thus, the data for two groups of cells were combined. On average, the bAP amplitude at the stimulation site, in this group of neurons, increased during paired activity by $45 \pm 9\%$ ($n = 17$). The inactivation of A-type potassium conductance caused by local EPSP-driven depolarization has been identified as an ionic mechanism responsible for the boosting of the bAP by paired activity (Magee & Johnston, 1995; Watanabe *et al.* 2002).

In 18 other cells, pairing a train of EPSPs with a bAP resulted in a reduction of the bAP amplitude at the stimulation site. A typical example is shown in Fig. 5*B* and *C*. In 8 neurons of this group, including the experiment shown in Fig. 5, the stimulating electrode was positioned on an oblique dendrite or on a branch that was distal to the main bifurcation of the apical trunk. In this group of cells the bAP amplitude at the stimulation site was reduced by paired activity by $45 \pm 9\%$ ($n = 8$). In the remaining 10 neurons the stimulation site was on the main apical trunk and the amplitude of the bAP was reduced, on average, by $18 \pm 2\%$ ($n = 10$). This amplitude reduction was significantly smaller compared with the previous group of cells ($P < 0.05$, two-population t test). Thus, the reduction of bAP with paired activity was significantly larger in oblique dendrites, compared with the apical trunk.

In the group of experiments in which paired activity did not alter the amplitude of bAP ($n = 9$), the stimulation site was on the apical dendrite in six cases. In the remaining three cells the stimulating electrode was positioned on an oblique dendrite or on a branch that was distal to the first bifurcation of the apical dendrite.

While the reduction in the bAP amplitude was significantly more pronounced in the oblique dendrites, we did not detect a correlation between the polarity of the effect (boosted or reduced bAP amplitude) and the location of activated synapses in the dendritic arbor. Further, we concluded from combined V_m and $[Ca^{2+}]_i$ measurements that the direction and the magnitude of the change in baseline-to-peak bAP amplitude, caused by paired pre- and post-synaptic activity, are spatially non-uniform and not directly related to the supra-linear summation of calcium signals. The quantitative relationship between these two variables during paired activity is described below, after the analysis of the composition of the Ca^{2+} signal.

Composition of calcium signal

The analysis of the correlation between V_m signals and Ca^{2+} signals relevant for the induction of LTP requires detection of the NMDA-dependent component of the calcium signal that serves as a link between V_m transients and the spine mechanism underlying LTP. Therefore, we examined the composition of the calcium signals by recording $[Ca^{2+}]_i$ transients in response to three stimulation protocols (bAP, EPSP train, paired stimulation) in the control solution and in the presence of a saturating concentration of AP-5 (50–100 μM; Watkins & Evans, 1981) introduced into the bath to block Ca^{2+} influx mediated by NMDA receptors. The drug greatly reduced the slow, NMDA-R-dependent component of the EPSP train (Fig. 5*H*). In hippocampal slices, the concentration of 25–100 μm AP-5 has been repeatedly shown to produce an essentially total but reversible blockade of NMDA-R-mediated Ca^{2+} transients measured at the level of individual spines (e.g. Emptage *et al.* 1999; Kovalchuk *et al.* 2000; Nevian & Sakmann, 2004). Thus, the residual $[Ca^{2+}]_i$ signal in the AP-5 solution was interpreted as the non-NMDA-R-dependent component of the composite signal. The NMDA-dependent component was obtained by subtracting the residual $[Ca^{2+}]_i$ signal from the total signal.

Figure 5*F* and *G* illustrates typical measurements. The colour-coded relative spatial maps of the peak $[Ca^{2+}]_i$ signal and actual recordings from five selected regions are shown in Fig. 5*F*. The first three panels from the top show $[Ca^{2+}]_i$ signals generated in response to three stimulation protocols (bAP alone, EPSP train alone, paired activity). In this measurement, as already shown for the experiment in Fig. 4, paired activity generated a marked supra-linear increase in $[Ca^{2+}]_i$ transient at the site of stimulation (third panel from top). The supra-linear component of the signal (bottom panel) was isolated using the subtraction procedure described above. The relative spatial map of the peak signal indicated that the supra-linear component of the calcium change was restricted to the site of stimulation and strictly correlated spatially to the EPSP response. After addition of the NMDA blocking agent AP-5 (Fig. 5*G*), the $[Ca^{2+}]_i$ signal related to the bAP which is mediated by voltage-sensitive calcium channels, was unaltered (top panel). The response to synaptic stimulation (second panel from top), which was small and at the limit of recording resolution in the control solution, was further reduced by AP-5, as expected for the synaptic $[Ca^{2+}]_i$ signal. The response to paired stimulation was reduced dramatically (third panel from top) indicating a substantial contribution of the NMDA-R Ca^{2+} flux to this component of the signal. No signal remained after the subtraction procedure. In this experiment the entire supra-linear component of the Ca^{2+} influx during paired activity was mediated by NMDA receptors. The large NMDA-dependent increase in $[Ca^{2+}]_i$ in dendritic spines would be likely to dominate the composite $[Ca^{2+}]_i$ signal in thin dendritic branches that have a high density of spines.

This result was not obtained in all cells. An example of an opposite extreme case is illustrated in Fig. 6*A–C* in which the VSCC-dependent $[Ca^{2+}]_i$ influx dominated the supra-linear part of the composite signal. The signal was present in a region close to the stimulating electrode and was essentially insensitive to AP-5 indicating that it was mediated by the flux of Ca^{2+} through VSCCs activated by augmented peak membrane depolarization caused by paired activity. A pronounced and localized increase in the peak membrane depolarization with pairing was indeed recorded by voltage imaging at the site of EPSP origin (Fig. 6*C*, location 3). Obviously, the peak depolarization depended on the size of the EPSP depolarization and on the amplitude of the bAP, as modified by paired activity. In addition, the pairing-evoked change in bAP baseline-to-peak amplitude at a given site should be a function of the EPSP depolarization. This relationship was confirmed by comparing the boosting effect of a large EPSP depolarization (Fig. 6*D*, red traces) to the effect of a smaller depolarization (Fig. 6*D*, blue traces) at the same dendritic site. The smaller EPSP depolarization (produced by reducing the stimulus intensity) resulted in a larger boosting of bAP baseline-to-peak amplitude so that the total, peak depolarization remained approximately the same. Traces on the right show the comparison of the baseline-to-peak amplitude of the bAPs evoked alone (black trace) and during pairing with large (red trace) and small (blue trace) EPSP depolarization. Similar results were seen in all seven neurons tested.

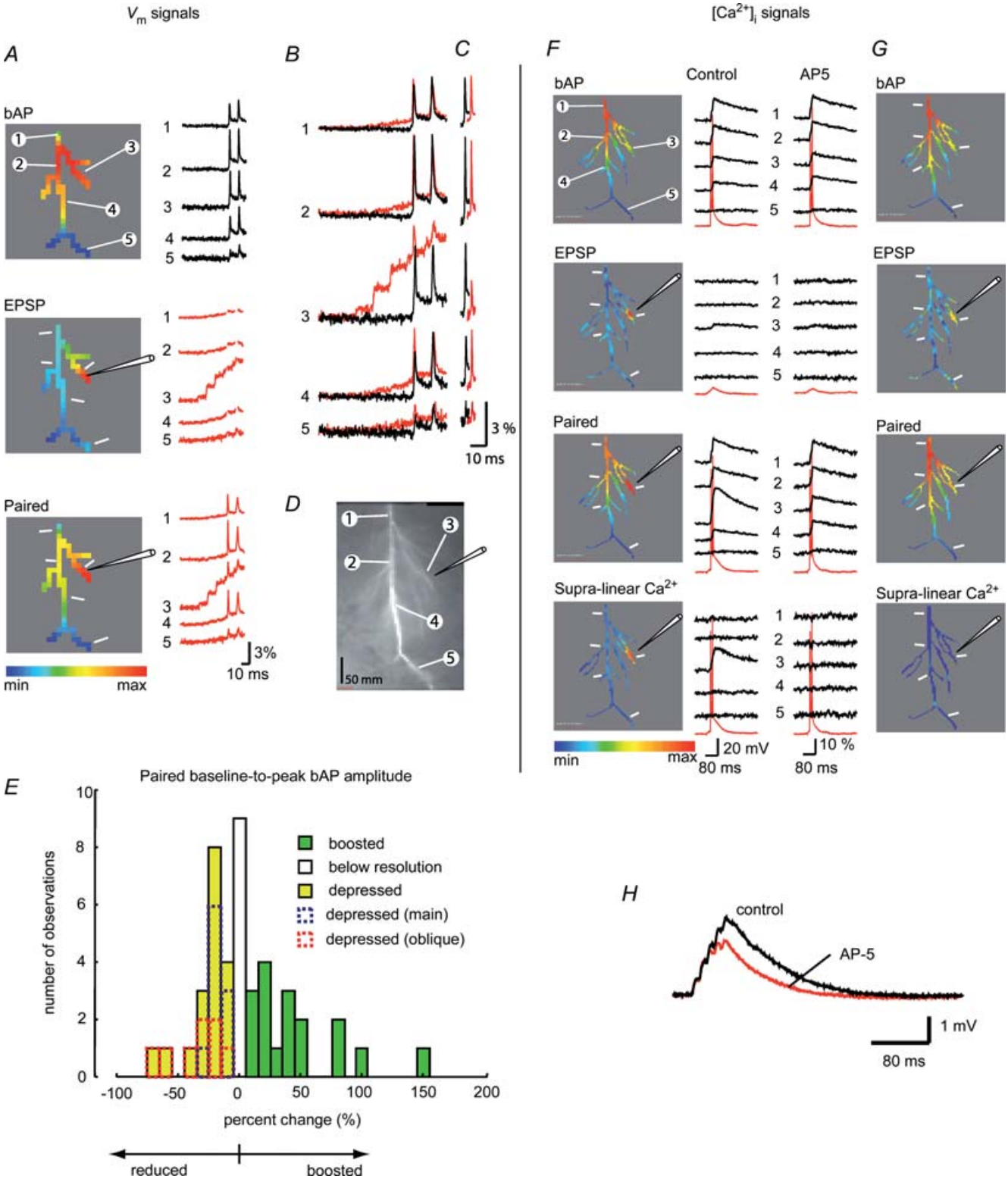

Figure 5. Boosting of bAP amplitude was not directly correlated with the NMDA-dependent component of the supra-linear calcium change evoked by LTP-forming stimuli

A, V_m signals: recordings during the three stimulation protocols (bAP, EPSP train, paired activity). The colour-coded relative spatial maps shown on the left; corresponding trace displays of signals from 5 representative locations shown on the right. To isolate parts of the recording used to generate a spatial map of the peak EPSP signal, spike signals were removed artificially in the middle panel (EPSP). *B*, V_m signals related to bAP (black traces) are superimposed with paired EPSP–bAP signals (red traces) to reveal region-specific changes in the peak membrane

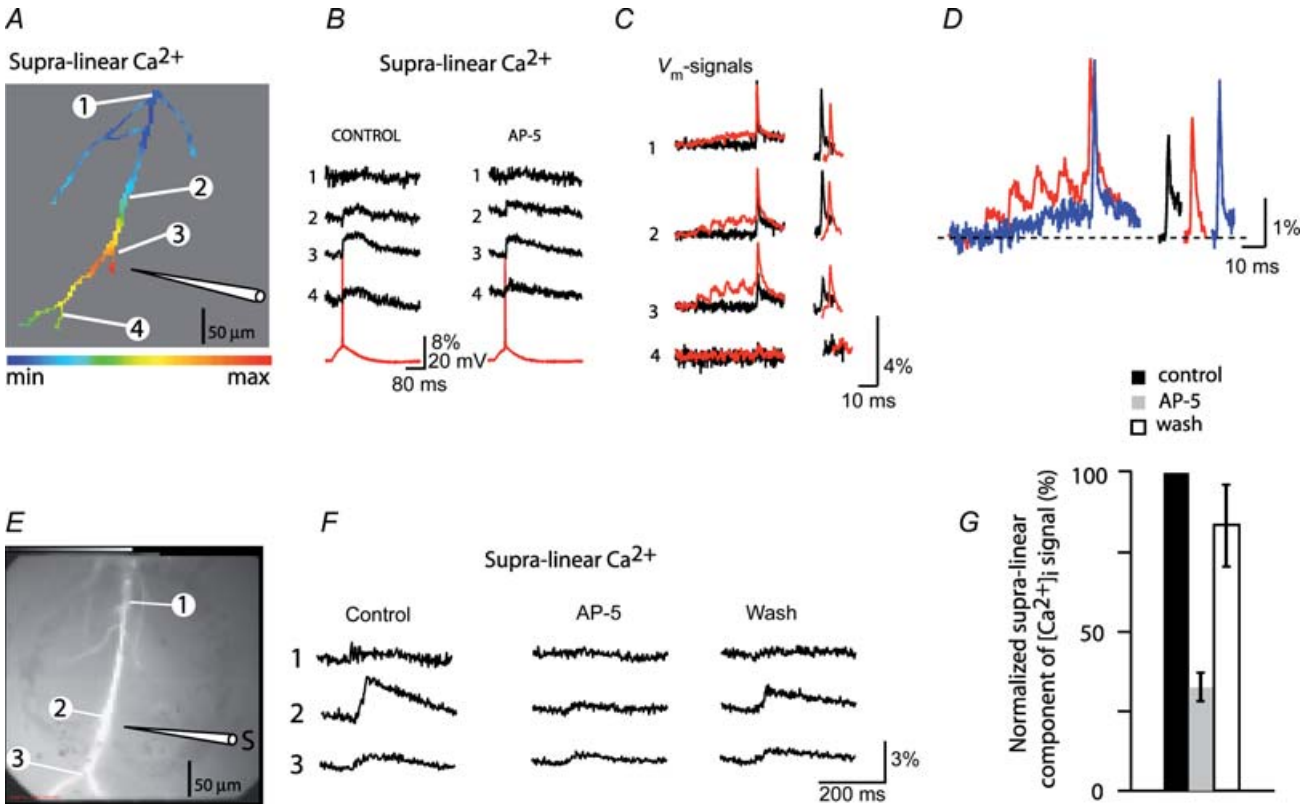

Figure 6. NMDA-dependent Ca^{2+} influx constituted, on average, 68% of the supra-linear component of the recorded signal evoked by LTP-forming stimuli
A, the relative spatial map of the supra-linear signal during paired activity in control solution. *B*, recordings of the supra-linear calcium signal from 4 selected locations in control solution and with 100 μm AP-5 present in the bath; the somatic V_m recordings shown in red. AP-5 did not influence supra-linear calcium signals in this experiment indicating that they were mediated by VSCCs. *C*, superimposed V_m signals from same 4 locations during bAP (black traces) and during paired EPSP–bAP signals (red traces) indicate region-specific changes in the peak membrane depolarization during paired activity. Traces on the right (shifted horizontally with respect to each other for clarity) are spike signals aligned to reveal region-specific differences in bAP baseline-to-peak amplitudes. *D*, traces on the left, peak membrane depolarization during pairing of bAPs with large (red trace) and small (blue trace) EPSP depolarization at location 3. Traces are slightly shifted horizontally with respect to each other for clarity. Traces on the right, bAP signals aligned to indicate the difference in baseline-to-peak amplitude; reduced depolarization (blue trace) clearly increased the boosting effect. Black trace, bAP evoked alone. *E*, dendritic arbor of another neuron in which both sources of calcium (NMDA-R dependent and VSCC dependent) contributed significantly to the composite signal. *F*, recordings of supra-linear $[Ca^{2+}]_i$ signals from 3 selected locations under control conditions, in the presence of 100 μm AP-5 in the bath, and after wash-out of the drug. *G*, summary plot of the normalized decrease in signal amplitude in the presence of AP-5 ($n = 13$) and the effect of the wash-out of the drug ($n = 5$).

depolarization. *C*, bAP signals aligned with paired EPSP–bAP signals to reveal region-specific differences in action potential threshold to the peak amplitudes (EPSP signals subtracted). Traces are shifted horizontally with respect to each other for clarity. *D*, fluorescent images of the dendritic arbor (bis-fura-2 excitation); five recording regions (1–5) and the stimulating electrode position are indicated. *E*, frequency distribution histogram of the change in the bAP baseline-to-peak amplitude evoked by LTP-forming stimuli. Green bars, boosting ($n = 17$). White bar, no change ($n = 9$). Yellow bars, depression ($n = 18$). Dendritic stimulus location: blue, apical trunk ($n = 10$); red, oblique or apical branch ($n = 8$). *F* and *G*, $[Ca^{2+}]_i$ signals during the three stimulation protocols in control solution and in the presence of 100 μm of AP-5 in the bath. The spatial maps of the peak signal shown on the left; corresponding trace displays are shown on the right with the somatic V_m traces shown in red. AP-5 completely eliminated supra-linear component of the calcium signal in this experiment. *H*, somatically recorded EPSP train under control conditions and in the presence of 100 μm AP-5.

The relatively large diameter of the dendritic trunk (compared with oblique dendrites) and a relatively low density of activated spines could explain why the NMDA-dependent fraction of the non-linear $[Ca^{2+}]_i$ signal was not recorded in this experiment. In our measurements we expected to detect the NMDA-R-mediated $[Ca^{2+}]_i$ signal from thin dendrites with high density of spines but not from a thick dendritic branch in which the ratio of spine volume to shaft volume is very small. It is plausible to assume however, that the physiological process that takes place in dendritic spines during paired activity is identical in both cases.

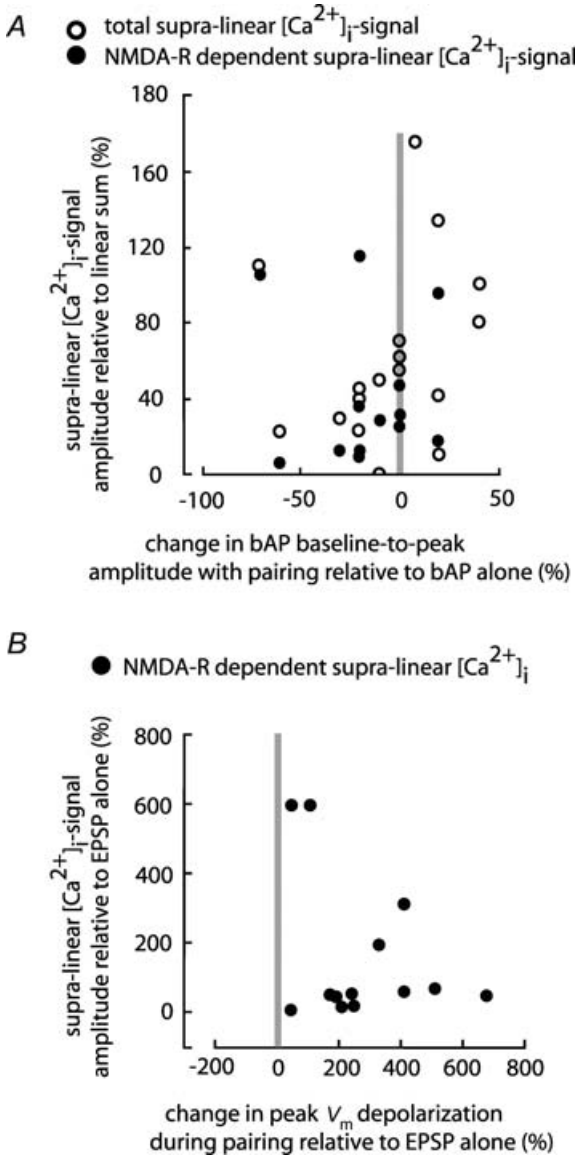

Figure 7. Correlation between V_m signals and $[Ca^{2+}]_i$ transients during paired activity
A, scatter-plot of the supra-linear $[Ca^{2+}]_i$ signal (○) and its NMDA component (●) *versus* change in bAP baseline-to-peak amplitudes evoked by paired activity does not show significant correlation (correlation coefficients, $r = 0.0984$ and -0.0675; $P > 0.5$). *B*, scatter-plot of the change in the NMDA-R-dependent component of the supra-linear $[Ca^{2+}]_i$ signal *versus* change in the peak V_m depolarization. The signals evoked by paired activity are expressed relative to the signals recorded during EPSP stimulation alone. $r = 0.3319$; $P > 0.2$.

One or the other pathway for calcium entry appears dominant in the two experiments shown in Figs 5, and 6*A–C*. In most cases, however, both sources of calcium contributed significantly to the composite signal. The results from one of those experiments are shown in Fig. 6*D* and *E*. The measurements of $[Ca^{2+}]_i$ transients in response to three stimulation protocols were carried out under control conditions, with AP-5 added to the bath, and after the drug was washed out (recovery period of 20 min in control solution). Only the supra-linear component of the composite $[Ca^{2+}]_i$ signal is shown in Fig. 6*E*. In this experiment, the supra-linear signal was reduced by approximately 80% in AP-5. The residual signal apparently represents the flux of Ca^{2+} mediated by VSCC. This result reflects the contribution of NMDA-dependent Ca^{2+} influx in activated dendritic spines to the total intracellular volume in which the composite signals were monitored. The summary of all 13 experiments showing the effect of AP-5 is plotted in Fig. 6*F*. On average, AP-5 reduced the supra-linear component of the composite $[Ca^{2+}]_i$ signal by $68 \pm 8\%$ ($n = 13$). The effect of the washout of the drug was determined in five neurons. In these experiments the AP-5-induced block was largely reversible ($85 \pm 13\%$; $n = 5$).

Correlation between V_m signals and $[Ca^{2+}]_i$ transients

Clearly, because of the limited spatial resolution, our assay does not measure directly NMDA-R-mediated supra-linear $[Ca^{2+}]_i$ signals in the spines. Instead, we monitored a composite signal which would be expected to vary at different stimulation sites as a function of both the density of activated spines and the volume of the dendritic branch monitored. These factors could not be determined in our experiments and, thus, the amplitude of the supra-linear $[Ca^{2+}]_i$ signals could not be used as a reliable quantitative variable in characterizing the relationship between the relative change in V_m signals during paired activity and the induced $[Ca^{2+}]_i$ signals at different dendritic sites. Nevertheless, two important conclusions can be derived from the qualitative analysis of the results, as shown in Fig. 7.

First, we conclude that the direction and the magnitude of the change in baseline-to-peak bAP amplitude, caused by paired pre- and post-synaptic activity, were not directly related to the supra-linear summation of calcium signals. The relationship between these two variables during paired activity is shown in Fig. 7*A*. Both the total supra-linear Ca^{2+} signal (open circles) and the NMDA-R-dependent

component are plotted against the relative change in baseline-to-peak bAP amplitude caused by paired activity. Both the increase and the decrease in bAP amplitude were associated with an increase in $[Ca^{2+}]_i$ signal. The correlation coefficients for the total supra-linear calcium data and for the NMDA-dependent supra-linear calcium data were 0.0984 and −0.0675, respectively, indicating that the two variables are not correlated (with $P > 0.5$). Thus, the postsynaptic depolarization mandatory for the induction of supra-linear $[Ca^{2+}]_i$ signals did not require boosting of the bAP amplitude itself.

Second, the results show that the increase in the peak V_m depolarization during paired activity was required and, hence, directly related to the supra-linear summation of calcium signals. To illustrate this fact, the fractional increase in the NMDA-R-dependent supra-linear $[Ca^{2+}]_i$ signal evoked by paired activity, relative to the signal evoked by EPSP alone, is plotted as a function of the relative change in the peak V_m depolarization for 13 experiments in which the NMDA-R-dependent component of the supra-linear $[Ca^{2+}]_i$ signal was isolated using AP-5. (Fig. 7*B*). Unlike the amplitude of the bAP shown in Fig. 7*A*, the peak V_m depolarization preceding the supra-linear $[Ca^{2+}]_i$ signal was always augmented by paired activity. At the same time, the scatter-plot showed that two variables, as determined in 13 different neurons, are not correlated statistically (the correlation coefficients $r = 0.3319$; $P > 0.2$). This result, however, is not surprising given that the measurements of spine-related $[Ca^{2+}]_i$ signals were indirect and not quantitatively reliable (see Discussion).

Contrary to the NMDA-R-mediated $[Ca^{2+}]_i$ signal originating in dendritic spines, the AP-5-insensitive, VSCC-dependent component of the supra-linear $[Ca^{2+}]_i$ signal activated by the region-specific increase in the peak V_m depolarization during paired activity, should be strictly correlated with the spatial distribution of the recorded relative change in V_m. This prediction was confirmed. An example of the spatial correlation between the peak V_m depolarization and the VSCC-dependent supra-linear $[Ca^{2+}]_i$ signal from three different neurons and the summary result in the form of a scatter-plot for 13 experiments are shown in Fig. 8. Recordings in panel *A* illustrate the region-specific relative change in the peak V_m depolarization and the associated relative change in $[Ca^{2+}]_i$ signals in one neuron. The colour-coded representation of the data from the same cell (panels *B*) illustrate obvious spatial correlation between V_m signals

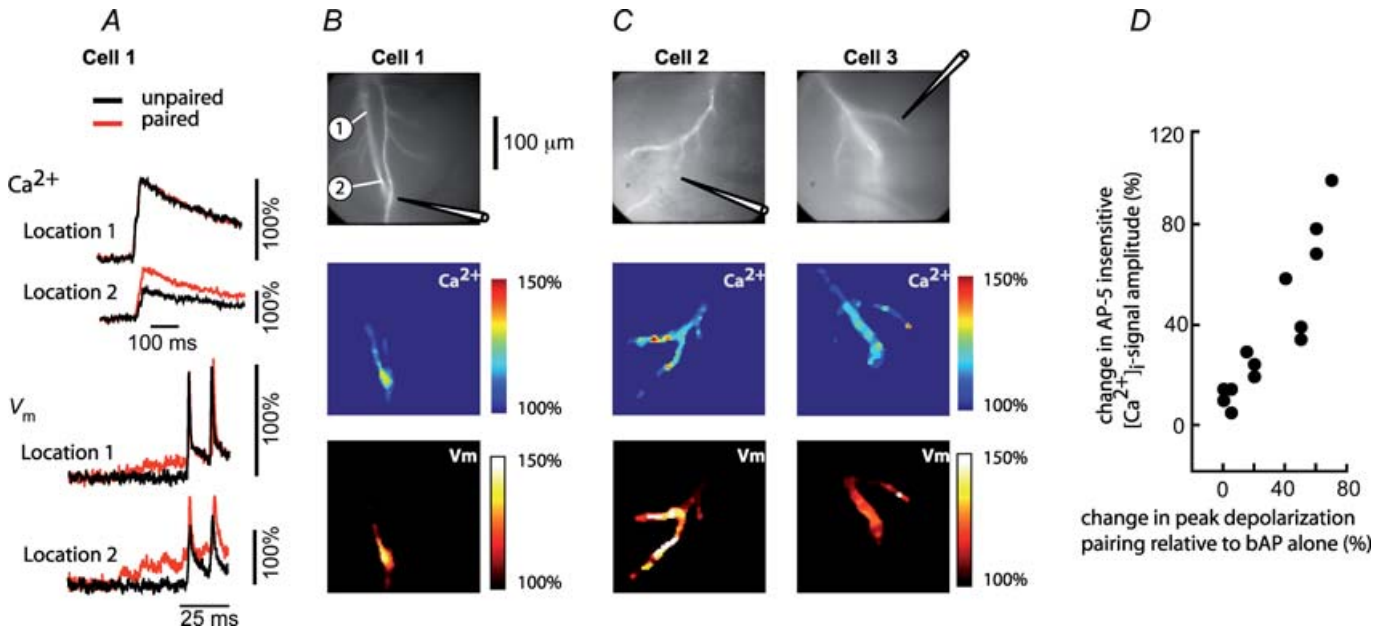

Figure 8. Spatial correlation between the amplitude of AP-5-insensitive component of the supra-linear $[Ca^{2+}]_i$ signal and the peak membrane depolarization during paired activity
A, $[Ca^{2+}]_i$ signals and V_m signals corresponding to bAPs (black traces) and paired EPSP–bAP signals (red traces) from two locations on the dendritic tree of Cell 1 shown in *B*. Signals are superimposed to reveal the region-specific increase in peak depolarization during paired activity. *B*, upper panel: fluorescence image of the dendritic arbor of Cell 1. The stimulating electrode is indicated schematically. Middle panel: colour-coded spatial map of the change in $[Ca^{2+}]_i$ signal amplitude during paired activity. Bottom panel: spatial map of the change in peak membrane depolarization (V_m) during paired activity. *C*, spatial correlation between V_m and $[Ca^{2+}]_i$ signal in two additional neurons. *D*, scatter-plot of the AP-5-insensitive $[Ca^{2+}]_i$ signal measured at the site of EPSP origin *versus* the change in peak membrane depolarization at the same location induced by paired activity. $r = 0.9$ ($P < 0.001$).

and $[Ca^{2+}]_i$ signals. Two additional examples of correlated spatial maps are shown in panel *C*. The correlation coefficient between the two variables in the scatter-plot (panel *D*) was 0.909 indicating a strong relationship (with $P < 0.001$, $n = 13$).

Discussion

We investigated V_m signals and $[Ca^{2+}]_i$ transients over large regions of the dendritic tree (220–400 μm distal to the soma) during coincident pre- and post-synaptic activity. Our analysis included oblique dendrites and distal apical branches where electrical signals have not been investigated before because dendritic patch-clamp recordings, so far, are not feasible on these structures. The central finding of our study is that unblocking of NMDA-Rs during coincident activity and the resulting supra-linear increase in Ca^{2+} influx at the site of activated synapses did not require boosting of the bAP baseline-to-peak amplitude. Instead, the change in bAP baseline-to-peak amplitude caused by paired activity was spatially inhomogeneous and not directly related to the supra-linear summation of calcium signals, and by extrapolation to LTP induction.

Our results apply to the above specified part of the dendritic arbor; in CA1 pyramidal cells this dendritic region is dominated (in terms of LTP induction) by bAPs while synaptically evoked local dendritic Ca^{2+} spikes are precluded by action potentials that initiate in the axon at a lower threshold (Golding *et al.* 1999, 2002). More distal (> 400 μm) dendritic regions of CA1 pyramidal neurons are likely to exhibit different long-term plasticity rules based on dendritic Ca^{2+} spikes (Golding *et al.* 2002; Lisman & Spruston, 2005). In layer V neocortical pyramidal neurons, however, bAPs were recently reported to have wider influence on LTP induction that includes distal synapses in the apical tuft (Sjostrom & Hausser, 2006).

Interpretation of calcium signals

The analysis of V_m signals and related changes in $[Ca^{2+}]_i$ relevant for the induction of LTP implies recording of both types of signals from multiple dendritic locations. At the moment, voltage imaging with organic intracellular dyes is the only technique capable of monitoring V_m transients from dendrites of individual neurons at high spatial resolution and with adequate sensitivity. When this technique, using a CCD camera in the whole-field fluorescence mode, is combined with calcium measurements, the $[Ca^{2+}]_i$ signals on each pixel, in our experiments as well as in measurements from other laboratories (e.g. Golding *et al.* 2002; Nakamura *et al.* 2002; Frick *et al.* 2004), originate from dendritic areas much larger than individual spines. This has the advantage of simultaneously recording calcium changes over large regions of the dendritic tree that would not be obtained using recording techniques that have single spine resolution. The disadvantage is that the extrapolation from the composite $[Ca^{2+}]_i$ signals to calcium changes in individual spines is indirect. This problem does not exist in $[Ca^{2+}]_i$ imaging with single spine resolution using confocal fluorescence microscopy (Kovalchuk *et al.* 2000) or two-photon excitation fluorescence microscopy (Yuste & Denk, 1995; Nevian & Sakmann, 2004). However, the integration of these techniques with whole-field voltage imaging, although possible in principle, has not been achieved. At the same time, V_m imaging with single spine resolution and adequate sensitivity is still not available. A significant step in this direction is a recent report (Nuriya *et al.* 2006) showing a proof of principle that voltage-dependent second harmonic generation signals from individual spines can be recorded. However, low sensitivity of these measurements required extensive averaging (280 trials) and resulted in large spine-to-spine variability that could not be explained. The difficulties of recording fast (submillisecond) V_m transients from small volumes with non-linear microscopy are still considerable, mainly because of the relatively small number of photons collected per time-point and the resulting high relative shot noise. Thus, further improvements in the S/N of this technique are necessary to make accurate measurements from dendritic spines possible (see Dombeck *et al.* 2005).

The first prerequisite of our study was to establish if the NMDA-dependent component of the calcium signal that serves as a link between V_m transients and the spine mechanism underlying LTP can be detected using whole-field fluorescence microscopy. Some of the earlier measurements of calcium signals did not resolve the NMDA-dependent component, possibly because it was highly localized to individual spines that were spread out on main dendritic branches and possibly because the contribution of the NMDA-R-dependent signal was reduced by indicator dye saturation in the small volume of the spine heads (Regehr *et al.* 1989; Miyakawa *et al.* 1992; Markram & Sakmann, 1994; Magee & Johnston, 1997). Other studies that recorded supra-linear summation of $[Ca^{2+}]_i$ signals did not attempt to determine its composition (e.g. Golding *et al.* 2002; Frick *et al.* 2003). On the other hand, Ca^{2+} entry through NMDA receptors on the oblique dendrites was clearly resolved in measurements similar to ours, as reported by Nakamura *et al.* (2002). In our experiments, the NMDA-dependent component of the calcium signal, isolated using pharmacological tools, was reliably resolved in the distal apical branches as well as in oblique dendrites. We could not establish, under our experimental conditions, whether NMDA-R-dependent component was amplified by calcium-induced calcium release as reported for CA1 pyramidal neurons in organotypic

cultures (Emptage *et al.* 1999; Emptage *et al.* 2003) and in slices (Raymond & Redman, 2006).

Under physiological conditions, in the absence of an indicator dye, the NMDA-R-dependent $[Ca^{2+}]_i$ transient, at least in some spines, is strictly localized to spine heads on the time scale of seconds because Ca^{2+} diffusion across the spine neck is negligible (Sabatini *et al.* 2002). Under our experimental conditions, however, the measurement of $[Ca^{2+}]_i$ signals requires an indicator dye which acts as a mobile buffer and potentiates significantly Ca^{2+} diffusion between dendrites and spines (by a factor of 10–100; Sabatini *et al.* 2002). In this sense, all measurements that use calcium indicator dyes underestimate the magnitude of the change in spine $[Ca^{2+}]_i$ because of the diffusion increase and because of the sublinear response of the indicator dye at high $[Ca^{2+}]_i$. This effect would be mitigated by using a lower affinity indicator dye. In several experiments ($n = 7$) we tested a low affinity dye, fura-6F, but could not derive useful information from these measurements because of the low S/N. Thus, the isolated NMDA-dependent component of the supra-linear bis-fura-2 $[Ca^{2+}]_i$ signal was detected in the non-linear range of the indicator. Nevertheless, the NMDA-dependent $[Ca^{2+}]_i$ signal that serves as a trigger for LTP is fully valid as an indicator used to identify region-specific calcium transients shown to be mandatory for persistent synaptic plasticity.

Interaction of V_m signals responsible for supra-linear Ca^{2+} transients

Our study provides experimental evidence for non-linear summation of V_m signals at the site of activated synapses that underlies the induction of supra-linear $[Ca^{2+}]_i$ transients. In agreement with previous studies, we recorded boosting of the baseline-to-peak bAP amplitude at some dendritic locations (Fig. 4*E* and *F*). However, the results obtained from one part of the dendritic tree were not valid for all regions – when synapses in different regions of the dendritic arbor were stimulated, bAPs were either unaffected, depressed or boosted while, at the same time, paired stimulation consistently produced NMDA-dependent supra-linear summation of $[Ca^{2+}]_i$ transients (Fig. 5*E*). Thus, boosting of bAP baseline-to-peak amplitude during paired activity was not critical for the induction of supra-linear $[Ca^{2+}]_i$ signals, and, by extrapolation, for LTP induction.

Backpropagating spikes have been identified as a critical retrograde signal to dendritic synapses in the induction of LTP (Markram *et al.* 1997; Magee & Johnston, 1997; Stuart & Hausser, 2001; Watanabe *et al.* 2002; Nevian & Sakmann, 2004; Sjostrom & Hausser, 2006; Kampa & Stuart, 2006). In this process, the change in synaptic strength depends critically on the timing of pre- and post-synaptic action potentials on the millisecond time scale (Markram *et al.* 1997; Sjostrom *et al.* 2001; Watanabe *et al.* 2002; Nevian & Sakmann, 2004). The mechanism for this timing requirement is not fully understood. The existing evidence suggests that the timing requirement is, at least partially, determined by the closing kinetics of the synaptic NMDA-R channels activated by glutamate (Nevian & Sakmann, 2004). The optimal interval during coincident activity, however, could also be based upon stringent timing requirements for non-linear summation of EPSPs and axonally initiated bAPs. Consistent with this idea were the results of several studies, carried out using dendritic recordings of V_m signals from the main apical trunk, which led to the conclusion that the regional bAP boosting participates in the control of supra-linear summation of $[Ca^{2+}]_i$ transients that trigger LTP. It was obvious in these experiments that localized EPSPs and decremental bAPs in the main dendritic apical trunk may interact in a supra-linear fashion because of the non-linear relation between membrane potential and voltage-sensitive ionic conductances that underlie the bAP. These studies suggested that bAP signals were based on a mixture of active and passive ionic currents with the proportion of these two components varying with membrane potential and the distance of the dendritic location from the soma (Stuart & Hausser, 2001; Bernard & Johnston, 2003). The passive component of the bAP would be expected to attenuate during paired activity because the distal EPSP-induced depolarization would decrease the voltage gradient responsible for the electrotonic current. This effect would contribute to sublinear summation. On the other hand, the regenerative component of the bAP is mainly determined by the voltage-dependent Na^+ and K^+ channels. The EPSP-induced depolarization would activate fast-inactivating Na^+ and A-type K^+ channels as well as non-inactivating K^+ channels. The net effect on bAP amplitude would depend on the density and activation and inactivation characteristics of these channels. In CA1 pyramidal neurons, the dominant ionic mechanism responsible for bAP amplitude boosting was identified as local inactivation of A-type K^+ channels by subthreshold synaptic activity (Hoffman *et al.* 1997; Magee & Johnston, 1997; Pan & Colbert, 2001; Watanabe *et al.* 2002). This concept was supported by a multi-compartmental model (Migliore *et al.* 1999). A similar boosting effect in the distal dendrites of neocortical pyramidal cells was found to be based on the dominant role of the EPSP-induced activation of voltage-gated Na^+ and Ca^{2+} channels (Williams & Stuart, 2000; Larkum *et al.* 2001; Stuart & Hausser, 2001; Sjostrom & Hausser, 2006). In both neocortical and pyramidal neurons, the boosting of bAPs by EPSPs was recognized as a mechanism that could play a critical role in the induction of associative forms of synaptic plasticity.

At the same time, the non-linear summation of EPSPs and bAPs in the entire dendritic arbor should, in principle,

have different size and polarity in different dendritic regions, changing with the amplitude of both signals as they vary from one location to another. Our results are consistent with this expectation. Also, consistent with our findings is a modelling study indicating that the conditions for supra-linear summation of EPSPs and bAPs in CA1 pyramidal neurons will be satisfied in a very limited number of synapses (approx. 10%) depending on their location on the dendritic tree. In the model, at the other 90% of synaptic sites, the summation of EPSP and bAP signals was predicted to be either linear or sublinear (Urakubo *et al.* 2004). Sub-linear summation of dendritic V_m signals has not been described explicitly prior to our study. However, a clear reduction in the baseline-to-peak amplitude of the bAP, similar to our findings, has been reported before in experiments on CA1 pyramidal neurons (see Fig. 1*B* in Pan & Colbert, 2001). The localized reduction in the baseline-to-peak amplitude of the bAP with pairing could be explained either by the EPSP-induced attenuation of the passive component of the bAP as described above or by the inactivation of voltage-dependent Na^+ channels responsible for the upstroke of the regenerative bAP. In our experiments, the recorded attenuation of the bAP is most probably induced by the combination of both effects. The boosting effect, on the other hand, must depend on active membrane properties. Previous work identified local inactivation of A-type K^+ channels as a mechanism responsible for bAP boosting in CA1 pyramidal neurons (Hoffman *et al.* 1997; Magee & Johnston, 1997; Pan & Colbert, 2001; Watanabe *et al.* 2002).

In a recent work on layer V neocortical pyramidal neurons Sjostrom & Hausser (2006) demonstrated a close correlation between local bAP boosting in the main dendritic apical shaft (recorded by patch-electrodes) and LTP induction in the thin dendritic branches of the distal apical tuft (where dendritic patch-clamp recording is not possible). This result could suggest that bAP boosting at the site of activated synapses might be required for LTP induction. However, recordings of membrane potential signals from the distal dendritic tuft branches are not available and our results demonstrate clearly that: (a) boosting of the bAP at one dendritic location can often be accompanied by the reduction of the bAP at another sites (see Fig. 5*C*), and (b) $[Ca^{2+}]_i$ transients are not a reliable indicator of the underlying interaction of membrane potential signals, at least in the dendrites of CA1 pyramidal neurons (see Fig. 3). Thus, direct evidence that boosting of the bAP is required at the site of activated synapses during LTP induction in the distal dendritic branches of the apical tuft in neocortical pyramidal neurons is lacking.

What could be the function of bidirectional bAP amplitude modulation at the site of activated synapses during paired activity? The role of bAP amplitude modulation is probably based on the relationship between the absolute magnitude of local dendritic depolarization and the magnitude of evoked supra-linear $[Ca^{2+}]_i$ transients. This relationship (Fig. 7*B*) could not be determined accurately in the present study because of the uncertainties in the measurements of the NMDA-R-mediated $[Ca^{2+}]_i$ signals that originate in spines. Nevertheless, this relation must be consistent with the voltage dependence of NMDA-R-mediated Ca^{2+} flux, as determined for forebrain neurons of the medial septum and CA1 pyramidal neurons (Schneggenburger *et al.* 1993; Garaschuk *et al.* 1996) as well as for individual spines of hippocampal neurons (Kovalchuk *et al.* 2000). According to this non-linear relationship (Fig. 9*B*), it would be incorrect to assume that amplification of the baseline-to-peak bAP amplitude always results in amplification of the $[Ca^{2+}]_i$ signal. Instead, Ca^{2+} influx through the open NMDA-R channel had a maximum at membrane potentials between 0 and −15 mV and became smaller at more negative and more positive values (Schneggenburger *et al.* 1993; Garaschuk *et al.* 1996; Kovalchuk *et al.* 2000). Therefore, the bAP with optimal amplitude in terms of LTP induction would depolarize the membrane to the range between −15 and 0 mV. This may require either boosting or the reduction of the bAP, depending on the initial size of both signals.

To illustrate this hypothesis, we approximately calibrated optical V_m signals in terms of membrane potential using the known absolute amplitude of the decremental bAP determined previously as a function of distance from the soma by dendritic electrode recordings (e.g. Frick *et al.* 2004). While this approximate calibration is the best available data at present, accurate calibration of localized V_m signals would be required for verification of this hypothesis. A method for the exact calibration of dendritic V_m signals has not been worked out. Optically recorded V_m transients are shown on the voltage scale for one experiment in Fig. 9. The resting membrane potential of −75 mV measured by somatic electrode was assumed to have the same value in the dendritic arbor. The bAP signal was approximated to be 60 mV in amplitude at dendritic site 1 in Fig. 9*A* (200 μm from soma) and 30 mV in amplitude at dendritic site 2 (300 μm from soma). The EPSP–AP pairing was evoked either at location 1 or at location 2 in different measurements using one of the two extracellular electrodes positioned as indicated in Fig. 9*A*. Local V_m signals from stimulated regions are shown in Fig. 9*B* and *C*. Signals obtained during unpaired and paired activity are superimposed. The steady-state voltage dependence of the Ca^{2+} flux through activated NMDA-Rs, adapted from Garaschuk *et al.* (1996), is shown on the same voltage scale (dashed curve on the right). Figure 9*B* indicated that the observed reduction in baseline-to-peak bAP amplitude (to 37%; inset) during paired activity resulted in a peak membrane depolarization

that closely matched the optimal range for the Ca^{2+} flux through activated NMDA-Rs (grey area). Without the reduction in the bAP amplitude during pairing the membrane potential would have overshot the optimal range significantly. At location 2 (Fig. 9*C*), contrary to the previous case, pairing resulted in boosting of bAP amplitude (to 125%). At this location, however, because of the size of both signals, boosting of bAP amplitude brought total membrane depolarization closer to the optimal range. In this context, bidirectional modulation of bAP amplitude during paired activity might be viewed as a part of the dendritic mechanism that regulates NMDA-R-mediated Ca^{2+} influx.

The above hypothesis implies that, at a given location, the change in bAP baseline-to-peak amplitude is a function of the EPSP depolarization. This relationship was confirmed, as shown in Fig. 6*D*.

Relevance for LTP

Our analysis of dendritic signals during one cycle of paired pre- and post-synaptic activity is similar to the previous studies designed to investigate localized interaction of signals responsible for LTP induction (Magee & Johnston, 1997; Pan & Colbert, 2001; Stuart & Hausser, 2001; Watanabe *et al.* 2002; Waters *et al.* 2003; Sjostrom & Hausser, 2006; Nevian & Sakmann, 2006). These studies contributed to the understanding of the mechanisms responsible for LTP induction, including synaptic modulation of bAP amplitude and the potential consequences for long-term plasticity.

However, the question of how interactions of V_m signals and associated Ca^{2+} transients recorded during one cycle of a pairing protocol are related to the effect of the complete LTP-inducing protocol composed of many cycles did not

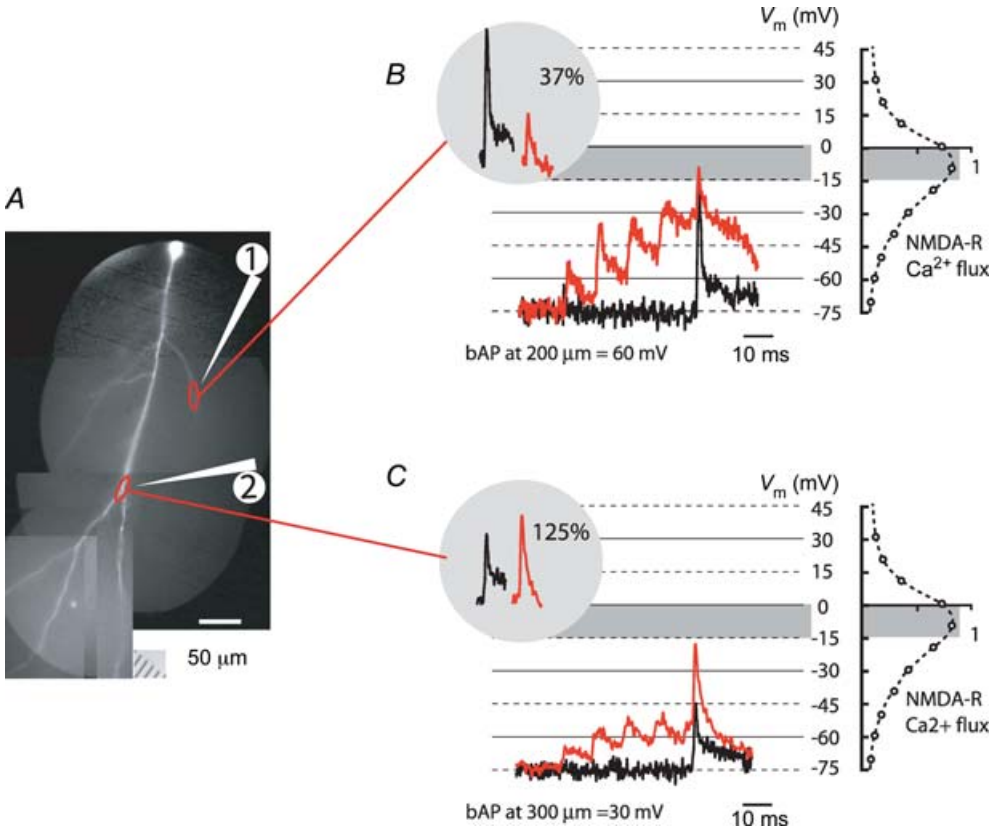

Figure 9. Non-linear summation of V_m signals during paired activity brings membrane potential to the optimal range for NMDA-R-mediated Ca^{2+} flux
A, a composite fluorescent image of a neuron. Position of two extracellular stimulating electrodes indicated schematically. *B*, superimposed V_m signals related to bAP evoked alone (black trace) and during paired activity (red traces) recorded from location 1 marked by upper red oval. The calibration of optical signals is approximate (see text). Baseline-to-peak bAP amplitude was reduced to 37% (left inset) by paired activity. The resultant peak membrane depolarization closely matched the range that corresponds to the maximum Ca^{2+} flux through activated NMDA-R (grey area). Voltage dependence of the Ca^{2+} flux through NMDA receptor channels (dashed trace; scale in arbitrary units) adapted from Garaschuk *et al.* (1996) is shown on the right. *C*, baseline-to-peak bAP amplitude, recorded from location 2 marked by lower red oval, was boosted to 125% (left inset) by paired activity. The resultant peak membrane depolarization was brought closer to the optimal range by bAP boosting at location 2.

receive adequate attention in general, and the available information is limited.

A recent study by Raymond & Redman (2006) provided a fresh insight into that question, showing that the number of repetitions of a theta-burst protocol applied to CA1 pyramidal neurons determines the type of induced LTP. Different LTP types appeared to be triggered by Ca^{2+} signals from different sources.

The role of prolonged high-frequency stimulation, however, and the role of repetitive theta-burst protocols in LTP induction seem to be complex. First, certain stimulation protocols were found to induce long-term changes in synaptic efficiency even after single application (Rose & Dunwiddie, 1986; Holthoff *et al.* 2004), without a need for repetitive stimulation. In other studies, the effect of repeated stimulation was clearly recorded (Huang & Kandel, 1994; Raymond & Redman, 2002, 2006) but the underlying mechanism that sets the threshold for LTP induction is not fully understood. A recent study (Nevian & Sakmann, 2006) carried out on layer 2/3 neocortical pyramidal neurons compared the measurements of spine $[Ca^{2+}]_i$ transients evoked by one cycle of paired activity with the recordings from the same spine during 60 repetitions of the same cycle. No correlation between the peak $[Ca^{2+}]_i$ amplitude and the number of pairings was found. The question that remained unresolved is why are 60 pairing repetitions needed to induce plasticity. At the same time, Petrozzino *et al.* (1995) reported that $[Ca^{2+}]_i$ in dendrites and spines increases gradually during 1 s tetanic stimulation indicating that the late increase in $[Ca^{2+}]_i$ might be critical for LTP induction. Obviously, the results from experiments which used different induction protocols, different types of neurons and different measurement techniques are difficult to compare. Nevertheless, it is clear that the role of repetitive stimulation is both complex and not adequately explored. The analysis of the interaction of local V_m and $[Ca^{2+}]_i$ transients during one cycle of the theta-burst protocol is a critical step toward characterizing mechanisms responsible for LTP induction. Full understanding of these mechanisms will ultimately require the analysis of the role of repetitive stimulation.

References

Antic S (2003). Action potentials in basal and oblique dendrites of rat neocortical pyramidal neurons. *J Physiol* **550**, 35–50.

Antic S, Major G & Zecevic D (1999). Fast optical recordings of membrane potential changes from dendrites of pyramidal neurons. *J Neurophysiol* **82**, 1615–1621.

Antic S, Wuskell JP, Loew L & Zecevic D (2000). Functional profile of the giant metacerebral neuron of helix aspersa: temporal and spatial dynamics of electrical activity in situ. *J Physiol* **527**, 55–69.

Antic S & Zecevic D (1995). Optical signals from neurons with internally applied voltage-sensitive dyes. *J Neurosci* **15**, 1392–1405.

Bekkers JM & Stevens CF (1990). Presynaptic mechanisms for long-term potentiation in the hippocampus. *Nature* **346**, 724–729.

Bernard C & Johnston D (2003). Distance-dependent modifiable threshold for action potential back-propagation in hippocampal dendrites. *J Neurophysiol* **90**, 1807–1816.

Bliss TV & Collingridge GL (1993). A synaptic model of memory: long-term potentiation in the hippocampus. *Nature* **361**, 31–39.

Chang PY & Jackson MB (2006). Heterogeneous spatial patterns of long-term potentiation in rat hippocampal slices. *J Physiol* **576**, 427–443.

Djurisic M, Antic S, Chen WR & Zecevic D (2004). Voltage imaging from dendrites of mitral cells: EPSP attenuation and spike trigger zones. *J Neurosci* **24**, 6703–6714.

Dombeck DA, Sacconi L, Blanchard-Desce M & Webb WW (2005). Optical recording of fast neuronal membrane potential transients in acute mammalian brain slices by second-harmonic generation microscopy. *J Neurophysiol* **94**, 3628–3636.

Emptage N, Bliss TV & Fine A (1999). Single synaptic events evoke NMDA receptor-mediated release of calcium from internal stores in hippocampal dendritic spines. *Neuron* **22**, 115–124.

Emptage NJ, Reid CA, Fine A & Bliss TV (2003). Optical quantal analysis reveals a presynaptic component of LTP at hippocampal Schaffer associational synapses. *Neuron* **38**, 797–804.

Frick A, Magee J & Johnston D (2004). LTP is accompanied by an enhanced local excitability of pyramidal neuron dendrites. *Nat Neurosci* **7**, 126–135.

Frick A, Magee J, Koester HJ, Migliore M & Johnston D (2003). Normalization of Ca^{2+} signals by small oblique dendrites of CA1 pyramidal neurons. *J Neurosci* **23**, 3243–3250.

Garaschuk O, Schneggenburger R, Schirra C, Tempia F & Konnerth A (1996). Fractional Ca^{2+} currents through somatic and dendritic glutamate receptor channels of rat hippocampal CA1 pyramidal neurones. *J Physiol* **491**, 757–772.

Golding NL, Jung HY, Mickus T & Spruston N (1999). Dendritic calcium spike initiation and repolarization are controlled by distinct potassium channel subtypes in CA1 pyramidal neurons. *J Neurosci* **19**, 8789–8798.

Golding NL, Staff NP & Spruston N (2002). Dendritic spikes as a mechanism for cooperative long-term potentiation. *Nature* **418**, 326–331.

Helmchen F, Imoto K & Sakmann B (1996). Ca^{2+} buffering and action potential-evoked Ca^{2+} signaling in dendrites of pyramidal neurons. *Biophys J* **70**, 1069–1081.

Hoffman DA, Magee JC, Colbert CM & Johnston D (1997). K^+ channel regulation of signal propagation in dendrites of hippocampal pyramidal neurons. *Nature* **387**, 869–875.

Holthoff K, Kovalchuk Y, Yuste R & Konnerth A (2004). Single-shock LTD by local dendritic spikes in pyramidal neurons of mouse visual cortex. *J Physiol* **560**, 27–36.

Huang Y & Kandel ER (1994). Recruitment of long-lasting and protein kinase A–dependent long-term potentiation in the CA1 region of hippocampus requires repeated tetanization. *Learn Mem* **1**, 74–82.

Jaffe DB, Johnston D, Lasser-Ross N, Lisman JE, Miyakawa H & Ross WN (1992). The spread of Na^+ spikes determines the pattern of dendritic Ca^{2+} entry into hippocampal neurons. *Nature* **357**, 244–246.

Kampa BM & Stuart GJ (2006). Calcium spikes in basal dendrites of layer 5 pyramidal neurons during action potential bursts. *J Neurosci* **26**, 7424–7432.

Koester HJ & Sakmann B (1998). Calcium dynamics in single spines during coincident pre- and postsynaptic activity depend on relative timing of back-propagating action potentials and subthresh old excitatory postsynaptic potentials. *Proc Natl Acad Sci U S A* **95**, 9596–9601.

Kovalchuk Y, Eilers J, Lisman J & Konnerth A (2000). NMDA receptor-mediated subthreshold Ca^{2+} signals in spines of hippocampal neurons. *J Neurosci* **20**, 1791–1799.

Larkum ME, Zhu JJ & Sakmann B (2001). Dendritic mechanisms underlying the coupling of the dendritic with the axonal action potential initiation zone of adult rat layer 5 pyramidal neurons. *J Physiol* **533**, 447–466.

Linden DJ (1999). The return of the spike. Postsynaptic action potentials and the induction of LTP and LTD *Neuron* **22**, 661–666.

Lisman J & Spruston N (2005). Postsynaptic depolarization requirements for LTP and LTD: a critique of spike timing-dependent plasticity. *Nat Neurosci* **8**, 839–841.

Loew LW, Cohen LB, Dix J, Fluhler EN, Montana V, Salame G (1992). A naphthyl analog of the aminostyryl pyridinium class of potentiometric membrane dyes show consistant sensitivity in a variety of tissue, cell and model membrane preparations. *J Membr Biol* **130**, 1–10.

Magee JC & Johnston D (1995). Characterization of single voltage-gated Na^+ and Ca^{2+} channels in apical dendrites of rat CA1 pyramidal neurons. *J Physiol* **487**, 67–90.

Magee JC & Johnston D (1997). A synaptically controlled, associative signal for Hebbian plasticity in hippocampal neurons. *Science* **275**, 209–213.

Malenka RC, Kauer JA, Zucker RS & Nicoll RA (1988). Postsynaptic calcium is sufficient for potentiation of hippocampal synaptic transmission. *Science* **242**, 81–84.

Malenka RC & Nicoll RA (1999). Long-term potentiation – a decade of progress? *Science* **285**, 1870–1874.

Maravall M, Mainen ZF, Sabatini BL & Svoboda K (2000). Estimating intracellular calcium concentrations and buffering without wavelength ratioing. *Biophys J* **78**, 2655–2667.

Markram H, Lubke J, Frotscher M & Sakmann B (1997). Regulation of synaptic efficacy by coincidence of postsynaptic APs and EPSPs. *Science* **275**, 213–215.

Markram H & Sakmann B (1994). Calcium transients in dendrites of neocortical neurons evoked by single subthreshold excitatory postsynaptic potentials via low-voltage-activated calcium channels. *Proc Natl Acad Sci U S A* **91**, 5207–5211.

Migliore M, Hoffman DA, Magee JC & Johnston D (1999). Role of an A-type K^+ conductance in the back-propagation of action potentials in the dendrites of hippocampal pyramidal neurons. *J Comput Neurosci* **7**, 5–15.

Miyakawa H, Ross WN, Jaffe D, Callaway JC, Lasser-Ross N, Lisman JE & Johnston D (1992). Synaptically activated increases in Ca^{2+} concentration in hippocampal CA1 pyramidal cells are primarily due to voltage-gated Ca^{2+} channels. *Neuron* **9**, 1163–1173.

Nakamura T, Lasser-Ross N, Nakamura K & Ross WN (2002). Spatial segregation and interaction of calcium signalling mechanisms in rat hippocampal CA1 pyramidal neurons. *J Physiol* **543**, 465–480.

Neher E & Augustine GJ (1992). Calcium gradients and buffers in bovine chromaffin cells. *J Physiol* **450**, 273–301.

Nevian T & Sakmann B (2004). Single spine Ca^{2+} signals evoked by coincident EPSPs and backpropagating action potentials in spiny stellate cells of layer 4 in the juvenile rat somatosensory barrel cortex. *J Neurosci* **24**, 1689–1699.

Nevian T & Sakmann B (2006). Spine Ca^{2+} signaling in spike-timing-dependent plasticity. *J Neurosci* **26**, 11001–11013.

Nuriya M, Jiang J, Nemet B, Eisenthal KB & Yuste R (2006). Imaging membrane potential in dendritic spines. *Proc Natl Acad Sci U S A* **103**, 786–790.

Palmer LM & Stuart GJ (2006). Site of action potential initiation in layer 5 pyramidal neurons. *J Neurosci* **26**, 1854–1863.

Pan E & Colbert CM (2001). Subthreshold inactivation of Na^+ and K^+ channels supports activity-dependent enhancement of back-propagating action potentials in hippocampal CA1. *J Neurophysiol* **85**, 1013–1016.

Petrozzino JJ, Pozzo Miller LD & Connor JA (1995). Micromolar Ca^{2+} transients in dendritic spines of hippocampal pyramidal neurons in brain slice. *Neuron* **14**, 1223–1231.

Raymond CR & Redman SJ (2002). Different calcium sources are narrowly tuned to the induction of different forms of LTP. *J Neurophysiol* **88**, 249–255.

Raymond CR & Redman SJ (2006). Spatial segregation of neuronal calcium signals encodes different forms of LTP in rat hippocampus. *J Physiol* **570**, 97–111.

Regehr WG, Connor JA & Tank DW (1989). Optical imaging of calcium accumulation in hippocampal pyramidal cells during synaptic activation. *Nature* **341**, 533–536.

Rose GM & Dunwiddie TV (1986). Induction of hippocampal long-term potentiation using physiologically patterned stimulation. *Neurosci Lett* **69**, 244–248.

Ross WN, Salzberg BM, Cohen LB, Grinvald A, Davila HV, Waggoner AS & Wang CH (1977). Changes in absorption, fluorescence, dichroism, and birefringence in stained giant axons: optical measurement of membrane potential. *J Membr Biol* **33**, 141–183.

Sabatini BS, Oertner TG & Svoboda K (2002). The life cycle of Ca^{2+} ions in dendritic spines. *Neuron* **33**, 439–452.

Schneggenburger R, Zhou Z, Konnerth A & Neher E (1993). Fractional contribution of calcium to the cation current through glutamate receptor channels. *Neuron* **11**, 133–143.

Sjostrom PJ & Hausser M (2006). A cooperative switch determines the sign of synaptic plasticity in distal dendrites of neocortical pyramidal neurons. *Neuron* **51**, 227–238.

Sjostrom PJ, Turrigiano GG & Nelson SB (2001). Rate, timing, and cooperativity jointly determine cortical synaptic plasticity. *Neuron* **32**, 1149–1164.

Spruston N, Schiller Y, Stuart G & Sakmann B (1995). Activity-dependent action potential invasion and calcium influx into hippocampal CA1 dendrites. *Science* **268**, 297–300.

Stuart GJ & Hausser M (2001). Dendritic coincidence detection of EPSPs and action potentials. *Nat Neurosci* **4**, 63–71.

Urakubo H, Aihara T, Kuroda S, Watanabe M & Kondo S (2004). Spatial localization of synapses required for supralinear summation of action potentials and EPSPs. *J Comput Neurosci* **16**, 251–265.

Watanabe S, Hoffman DA, Migliore M & Johnston D (2002). Dendritic K-channels contribute to spike-timing dependent long-term potentiation in hippocampal pyramidal neurons. *Proc Natl Acad Sci U S A* **99**, 8366–8371.

Waters J, Larkum M, Sakmann B & Helmchen F (2003). Supralinear Ca^{2+} influx into dendritic tufts of layer 2/3 neocortical pyramidal neurons in vitro and in vivo. *J Neurosci* **23**, 8558–8567.

Waters J, Schafer A & Sakmann B (2005). Backpropagating action potentials in neurones: measurement, mechanisms and potential function. *Prog Biophys Mol Biol* **87**, 145–170.

Watkins JC & Evans RH (1981). Excitatory amino acid transmitters. *Annu Rev Pharmacol Toxicol* **21**, 165–204.

Williams SR & Stuart G (2000). Backpropagation of physiological spike trains in neocortical pyramidal neurons: implications for temporal coding in dendrites. *J Neurosci* **20**, 8238–8246.

Wu J-Y & Cohen LB (1993). Fast multisite optical measurement of membrane potential. In *A Practical Guide to Technology for Quantitative Real-Time Analysis*, ed. Mason WT, pp. 389–404. Academic Press, New York.

Yuste R & Denk W (1995). Dendritic spines as basic units of synaptic integration. *Nature* **375**, 682–684.

Zecevic D (1996). Multiple spike-initiation zones in single neurons revealed by voltage-sensitive dyes. *Nature* **381**, 322–325.

Acknowledgements

This work was supported by NIH grant RO1NS42739 and by Kavli Institute for Neuroscience, Yale University School of Medicine. We are grateful to Daniel Johnston, Jeffrey Magee and Andreas Frick for help with some of the initial experiments, to Larry Cohen for helpful comments on the manuscript, to Leslie Loew and Joe Wuskel for kindly providing dyes, and to Jovan Mijovic for the expert help with the optical apparatus. M.C. was partially supported by a Physiological Society travel grant.

Supplemental material

The online version of this paper can be accessed at:
DOI: 10.1113/jphysiol.2006.125005
http://jp.physoc.org/cgi/content/full/jphysiol.2006.125005/DC1
and contains one supplemental figure entitled:

The measurement of Ca^{2+} signals during a burst of 3 bAPs was in the linear range of the indicator dye.

This material can also be found as part of the full-text HTML version available from http://www.blackwell-synergy.com